This is a preprint, the final version is subject to change, of the American Mineralogist (MSA)
Cite as Authors (Year) Title. American Mineralogist, in press.
DOI: https://doi.org/10.2138/am-2018-6563

Revision 1

The crystal chemistry of the sakhaite–harkerite solid solution

R. JAMES EVANS,[1,*], LEE A. GROAT,[1] JAN CEMPÍREK,[2] RADEK ŠKODA,[2] EDWARD S. GREW,[3] AND CYRIELLE BERNARD[4]

[1]Department of Earth, Ocean and Atmospheric Sciences, University of British Columbia, Vancouver, British Columbia V6T 1Z4, Canada

[2]Masaryk University, Kotlářská 267/2, 611 37 Brno, Czech Republic

[3]Department of Earth Sciences, University of Maine, 5790 Bryand Global Sciences Center, Orono, Maine 04469-5790, U.S.A.

[4]Laboratoire de Géologie, Ecole Normale Supérieure, 24, rue Lhomond, Paris, France

[*]E-mail: rjamesevans@gmail.com

Abstract

Sakhaite, c. $Ca_{48}Mg_{16}(BO_3)_{32}(CO_3)_{16}(HCl,H_2O)_2$, is a rare rock-forming borate-carbonate mineral typically occurring in high-temperature, low-pressure calcareous skarns. It forms a complete solid solution with harkerite, c. $Ca_{48}Mg_{16}[AlSi_4(O,OH)_{16}]_4(BO_3)_{16}(CO_3)_{16}(HCl,H_2O)_2$. The solid solution can be described with the general formula

$$Ca_{48}(Mg,Fe,Mn)_{16}(CO_3)_{16}\,[Al_aSi_{5-a}\,(O,OH)_{16}]_y(BO_3)_{32-4y}\,(HCl,H_2O)_n$$

where $y_{max} = 8$ and $n_{max} = 16 - y$. In this study, we examine samples of sakhaite and harkerite from four localities worldwide: Titovskoye deposit, Sakha Republic, Russia (type locality for sakhaite); Solongo B deposit, Buryatia Republic, Russia; Camas Malag, Skye, Scotland (type locality for harkerite); as well as a sakhaite-like mineral from the Kombat Mine, Tsumeb, Namibia. Samples were characterized by electron microprobe analysis and single crystal X-ray diffraction. The Si:B ratios of the samples ranged from that of endmember sakhaite (containing B only) to that of endmember harkerite (Si:B = 1:1), with several intermediate compositions. All samples were deficient in B relative to the ideal composition, implying significant substitution for borate groups. The Si:Al ratio of silicate-containing samples ranged from the ideal 4:1 to 4:1.5, implying substitution of Al at the Si site.

Structures of 14 crystals were refined with $R1$ ranging from 3 to 7%. All crystals showed cubic symmetry (space group $Fd\bar{3}m$) except for a harkerite composition approaching the end member from Camas Malag, which showed rhombohedral symmetry (space group $R\bar{3}m$). The cubic unit cell parameter was found to increase linearly with increasing Si content, except for the sakhaite-like mineral from Tsumeb. This mineral was found to have significant substitution of Pb for Ca (0.4-0.5 apfu) and was poor in Cl, which in most sakhaite and harkerite samples occupies the interstitial site surrounded by four borate groups. This interstitial site in the Tsumeb samples

appears to instead be mainly occupied by H_2O, which may qualify the mineral as a distinct species.

Keywords: sakhaite, harkerite, solid solution, crystal structure

INTRODUCTION

The solid solution between sakhaite, ca. $Ca_{48}Mg_{16}(BO_3)_{32}(CO_3)_{16}(HCl,H_2O)_6$, and harkerite, ca. $Ca_{48}Mg_{16}[AlSi_4(O,OH)_{16}]_4(BO_3)_{16}(CO_3)_{16}(HCl,H_2O)_2$, is distinctive in that the substitution involves entire clusters of polyhedra, instead of one or two sites as is typical of most natural solid solutions. The sakhaite-harkerite series is close to unique in containing essential carbonate, borate, and silicate groups; among other minerals, only britvinite and the related mineral roymillerite (IMA No. 2016-061) contain all three of these anion complexes. Originally the main structural difference between sakhaite and harkerite was interpreted to be a partial substitution of isolated BO_3 triangles with isolated SiO_4 tetrahedra (Ostrovskaya et al. 1966; Davies and Manchin 1970). Subsequent crystallographic studies of synthetic sakhaite (Chichagov et al. 1974) and natural harkerite and sakhaite (Manchin and Miehe 1976; Giuseppetti et al. 1977; Yakubovich et al. 1978, 2005), as well as the anomalous sakhaite-like mineral reported by Dunn et al. (1990), have revealed a far more complex relationship, which induced us to undertake this study of the crystal chemistry of the sakhaite-harkerite series.

Sakhaite and harkerite have been described from 14 localities worldwide, of which 11 are skarns and other calcareous rocks formed at low pressures and high temperatures, whereas two are Mn-rich rocks metamorphosed under greenschist and amphibolite facies conditions, and one is a deep-seated granulite facies complex (e.g., Grew 1996; Grew et al. 1999).

PREVIOUS STRUCTURAL STUDIES

Ostrovskaya (1969) was the first to consider the structures of sakhaite and harkerite, making use of powder X-ray diffraction, chemical, and infrared data. However, the sakhaite structure (Fig. 1) was revealed only in single-crystal refinements of synthetic sakhaite (Chichagov et al. 1974) and of natural sakhaite from Solongo, Buryatia, Russia (Yakubovich et al. 1978). This structure was found to be a framework composed of columns of Ca polyhedra oriented in all three crystallographic directions. The other constituents, i.e., Mg octahedra, BO_3 and CO_3 triangles, occupy the interstices of the framework, leaving two types of cavities, the larger of which is partly occupied by H_2O groups. Neither refinement located Cl, which is present in the synthetic sakhaite (Nekrasov and Malinko 1973) as well as in the natural material. Manchin and Miehe (1976) and Giuseppetti et al. (1977) reported that harkerite has a similar structure, but with partial substitution of four BO_3 triangles by a zunylite-like aluminosilicate pentamer (Fig. 2). In endmember harkerite, this substitution is ordered, with layers of borate groups alternating with layers of aluminosilicate pentamers normal to one of the cubic body diagonals of the sakhaite unit cell (Fig. 3), a threefold axis of symmetry. This substitution results in decreased symmetry from $F4_132$ to $R\bar{3}m$, with the harkerite unit-cell volume being ~50% larger due to a doubling of the *c* parameter. The same substitution occurs without ordering in sakhaites with low Si contents. Both minerals were found to show a marked pseudo-symmetry in space group $Fd\bar{3}m$ (a = 14.7 Å). Chlorine was located in the smaller cavities (Giuseppetti et al. 1977).

Citing the limitations of X-ray diffraction instrumentation in the 1970s, Yakubovich et al. (2005) newly refined the crystal structure of the Solongo sakhaite, but in space group $Fd\bar{3}m$,

which is in accord with systematic absences of reflections. They proposed the following general formula for the series:

$$Ca_{48}(Mg,Fe,Mn)_{16}(CO_3)_{16}\{Al[SiO_3(O,OH)]_4\}_y(BO_3)_{32-4y} \cdot n(H_2O,HCl) \quad (1)$$

$Z = 1$ for $Fd\bar{3}m$ ($Z = 1.5$ for $R\bar{3}m$ to maintain consistency with the proposed formula), where $y_{max} = 8$ and $n \leq 16 - y$ (this is a correction to the formula as published in Yakubovich et al. 2005, where the subscript to the BO_3 group was given as $32 - y$.) At $y = 0$ this formula corresponds to the composition of synthetic sakhaite (Chichagov et al. 1974). Up to at least $y = 1.5$ the structure has cubic symmetry, but near $y = 2$, Yakubovich et al. (2005) reported the presence of weak reflections and peak shifts in powder diffraction patterns that indicate the presence of a pseudoperiod $a' = a/2$ and possibly presage rhombohedral symmetry. Tilley (1951) reported rhombohedral symmetry for harkerite ($y = 4$) from Scotland where the borate and aluminosilicate groups are ordered (Giuseppetti et al. 1977).

The main substitution described by the parameter y is the replacement of four independent BO_3 triangles (Fig. 2A) by a pentamer of tetrahedra composed of four SiO_4 tetrahedra sharing corners with a central AlO_4 tetrahedron (Fig. 2B),

$$\square(\square BO_3)_4 \rightarrow Al(OSiO_3)_4 \quad (2)$$

As this substitution is not charge-balanced as written, it must be accompanied by another substitution in the structure such as $O^{2-} \rightarrow OH^-$ or $M^{2+} \rightarrow M^{3+}$.

The tetrahedral pentamer is unusual in silicates, only known to occur in harkerite, in zunyite (Dirken et al. 1995) as Si_5O_{16}, and in rondorfite as $MgSi_4O_{16}$ (Mihajlović et al. 2004). Grew et al. (1999) found that in harkerite from the Isle of Skye, Crestmore Quarry in California, and Cascade Slide in New York, Al increased with Si in a ratio near 1:6 rather than the ideal 1:4, resulting in a substitution approaching

$$(BO_3)_4 \rightarrow (Al_{0.75}Si_{0.25})Si_4O_{15.25}(OH)_{0.75} \quad (3)$$

Note that this substitution is charge balanced.

Yakubovich et al. (2005) pointed out that compositions with $y > 4$, i.e., with SiO_4 tetrahedra dominant over BO_3 triangles, "should lead to the formation of new defects and structural order", and that at $y = 8$ (the borate-free composition) "one might expect a new ordered structure". Natural or synthetic compounds of compositions with $y > 4$ have yet to be found or synthesized.

Neutral H_2O and HCl molecules can be incorporated into small and large cavities in the structure (Yakubovich et al. 2005), but this has not been studied in any detail. The large cavities in sakhaite are surrounded by BO_3 triangles with an interstitial site near the center of the cavity partially occupied by H_2O or HCl. In harkerite half of the large cavities are occupied by the $Al(Si_4O_{16})$ groups (Fig. 2A). At most, $8 - y$ of the large cavity interstitial sites may thus be occupied per formula unit, although usually not all of these interstitial sites are occupied. An additional eight small cavities per formula unit could potentially host an additional interstitial site, but this has not been unambiguously observed in crystal structure refinements. Dunn et al. (1990) reported a highly hydrated sakhaite-like material from the Kombat Mine, Namibia, with a cubic space group and approximate composition $Ca_{48}Mg_{16}[AlSi_4(O,OH)_{16}]_{1.5}(BO_3)_{26}(CO_3)_{16}\cdot 14\text{-}16H_2O$, which may necessitate additional interstitial sites beyond those in the large cavities.

Yakubovich et al. (2005) also noted that Fe and Mn replace Mg at the Mg site, but representatives of this mineral family with dominance of either cation over Mg have yet to be found. Some replacement of Ca by rare earth elements (REEs) has also been reported (Barbieri et al. 1977, Galuskina et al. 2008). Some analyses have shown CO_3 in excess of the 16 per formula unit (pfu) of formula 1 (Machin and Miehe 1976; Barbieri et al. 1977). Machin and Miehe (1976)

suggested that the replacement of $(BO_3)_4^{12-}$ by $Al(SiO_4)_3^{13-}$ was charge-balanced by the replacement of an additional BO_3^{3-} by a CO_3^{2-} group.

EXPERIMENTAL

Samples from several world localities were obtained from a variety of sources (Table 1). All members of the sakhaite-harkerite series have been reported to fluoresce, thus all samples were initially examined with ultraviolet light. Polished thin sections of all samples were investigated with a petrographic microscope, and all samples were examined with a Philips XL30 scanning electron microscope (SEM) equipped with an energy-dispersion X-ray spectrometer (EDS) at the University of British Columbia.

Electron microprobe compositions were obtained from carbon-coated polished grain mounts with a Cameca SX100 electron microprobe at the Laboratory of Electron Microscopy and Microanalysis, Department of Geological Sciences, Masaryk University, Brno, in wavelength-dispersive mode. Content of elements with $Z \geq 9$ were measured using an accelerating voltage of 15 kV, a beam current of 10 nA, and a beam spot-size of 5 μm. The following standards and X-ray lines were used: topaz (F*K*α), albite (Na*K*α), olivine (Mg*K*α), sanidine (Al*K*α, Si*K*α, K*K*α), vanadinite (Cl*K*α, Pb*M*α), wollastonite (Ca*K*α), titanite (Ti*K*α), spessartine (Mn*K*α), almandine (Fe*K*α), fluorapatite (P*K*α), $SrSO_4$ (S*K*α, Sr*L*α), lammerite (As*L*α), yttrium-aluminum-garnet (Y*L*α), baryte (Ba*L*α), $LaPO_4$ (La*L*α), $CePO_4$ (Ce*L*α), and $NdPO_4$ (Nd*L*α). The peak counting time was 10 s for the majority of elements and 30 s for F and Pb. The background counting time was one-half of the peak counting time at the high- and low-energy background positions. Boron was analyzed in peak-area mode from a B*K*α line using a

danburite standard and accelerating voltage of 5 kV, beam current of 100 nA, beam diameter of 10 μm, and a Ni/C multilayered monochromator with $2d$ = 95 Å (CAMECA PC2). Peak-area integration was carried out in the range 62–74 Å for 120 s over 1000 steps. The first and the last 100 steps were used for background determination. Data were processed using the X-Phi matrix correction of Merlet (1994). The detection limit for B is ~2500 ppm and the relative error expressed as 3σ is ~10 relative% for 15 wt% B_2O_3 content. We chose to operate in peak-area mode because McGee and Anovitz (1996) showed that the effect of differences in the composition and structure of the standard and unknown on the shape and position of the B*K*α peak, especially the B coordination (tetrahedral in danburite, trigonal in the unknowns), is reduced when the peak area is measured. Interference of the B*K*α peak with the Cl*L*l and Cl*L*n lines was corrected using empirically determined correction factors. Carbon could not be analyzed due to the use of carbon coating on the samples to provide electrical conductivity, and due to CO_2 contamination of the vacuum chamber during analysis.

Single-crystal X-ray diffraction measurements were obtained in the Department of Chemistry at UBC using either a Bruker X8 diffractometer with graphite-monochromated Mo*K*α radiation or a Bruker DUO APEX II diffractometer with TRIUMPH monochromated Mo*K*α radiation. The data were collected at room temperature to maximum 2θ values between 55.1° and 89.6° for different crystals. Data were collected with a series of φ and ω scans in 0.50° oscillations with 10 to 20 s exposure depending on the strength of the diffraction spots. The crystal-to-detector distance was between 37.6 and 40.0 mm. Data were collected and integrated using the Bruker SAINT software package (Bruker 2007). The program CELL_NOW (Sheldrick 2008) was used to check for twinning and to separate reflections from different domains if twins

were present. Data were corrected for absorption effects using the multi-scan technique (SADABS, Sheldrick 1996) and were corrected for Lorentz and polarization effects.

All refinements were performed using the SHELXTL crystallographic software package (Sheldrick 2008) of Bruker AXS. Neutral atom scattering factors were taken from Cromer and Waber (1974). The weighting scheme was based on counting statistics. Anomalous dispersion effects were included in F_{calc} (Ibers and Hamilton 1964); the values for $\Delta f'$ and $\Delta f''$ were those of Creagh and McAuley (1992). The values for the mass attenuation coefficients are those of Creagh and Hubbell (1992). The crystal structures were initially solved and refined in space group $Fd\bar{3}m$ (cubic) or $R\bar{3}m$ (rhombohedral). Images of the post-refinement structures were drawn with the software VESTA 3.3 (Momma and Izumi 2011).

RESULTS

Fluorescence

All of the samples identified as being from the Sakha Republic in Russia exhibited a weak purple fluorescence in UV light. None of the other samples examined in this study fluoresced.

Compositions

Electron microprobe compositions for 13 single crystals are listed in Tables 2 and 3. Samples measured were HS1-D (135 × 150 μm), HS10-1 (270 × 755 μm), HS10-2 (410 × 240 μm), H10-3 (two crystallites 400-500 μm diameter), HS10-4 (605 × 250 μm), HS11-A (46 × 77 μm), HS11-B (50 μm diameter), HS11-C (five crystallites between 150 and 400 μm diameter), HS12-A (2100 × 250 μm), HS14-A (55 × 108 μm), HS14-B (50 μm dianmeter), HS14-C (two crystallites 90 × 165 μm and 65 × 120 μm), and HS15-B (165 × 140 μm). Note that some of

these crystals were also measured by single crystal diffraction, but not all, while some single crystal diffraction samples were not available for EMPA. Raw totals ranged from 78.6 to 83.1 oxide wt%, as CO_2 and H_2O, both significant components of sakhaite-harkerite, were not detectable by electron microprobe analysis (EMPA). The following structural formula, based on Equation 1 above, was used to calculate the compositions:

$$X_{48}\,Y_{16}\,Al_{ay}\,Si_{(5-a)y}\,B_{32-4y}\,C_{16}\,O^*_{144+4y}\,(HCl)_n \qquad (4)$$

where X = Ca, Na, K, Pb, Sr, Ba, or REEs; Y = Mg, Ti, Fe, or Mn; and O* = O, OH, or F. The EMPA data were normalized on 16 cations at the Y site for most compositions; if this normalization resulted in a total at the X site greater than 48, the formula was re-normalized based on 48 cations at the X site. Carbon was calculated based on 16 C per formula unit. Aluminum and silicon were assumed to substitute for each other at both sites of the aluminosilicate pentamer with no vacancies,

$$T^{Al}T^{Si}{}_4O^*{}_{16} = Al_{1+a}Si_{4-a}O^*{}_{16} \qquad (5)$$

where Al substitutes for Si if $a > 0$ and vice versa if $a < 0$; thus the number of pentamers per formula unit (y) was calculated as 1/5(Al + Si).

Assuming no vacancies at either the trigonal B site (T^B) or the tetrahedral Si site (T^{Si}), the structure requires

$$T^B + T^{Si} = 32 \qquad (6)$$

and a minimum of 144 + T^{Si} anions (O*) per formula unit (excluding Cl). Calculating T^{Si} as above, the boron content as determined by EMPA is too low by 5% to 45% (average 26%) to satisfy this structural requirement. The required boron content B* was calculated as 32 – T^{Si} = 32 – 4/5(Al + Si). All Cl in the structure was assumed to be present as HCl, and additional H_2O as OH was assumed to bring the anion total to 144 + T^{Si}.

DISCUSSION

The crystal structure of sakhaite-harkerite

The sakhaite structure is cubic with a unit cell parameter of approximately 14.7 Å. The structure is based on a framework of face-sharing $CaO_{9\text{-}11}$ (X) polyhedra. In the cubic structure there is one such symmetrically independent polyhedron which is stacked in columns parallel to the crystal axes (Fig. 1A). Each $CaO_{9\text{-}11}$ polyhedron sits at the intersection of three orthogonal columns. Small and large cavities in the framework are each surrounded by six $CaO_{9\text{-}11}$ polyhedra. The Mg (Y) site is six-coordinated and shares multiple faces with $CaO_{9\text{-}11}$ polyhedra (Fig. 1B); four Mg octahedra border the small cavity, but none border the large cavity.

The triangular borate and carbonate groups reinforce the Ca-Mg framework, sharing edges with the $CaO_{9\text{-}11}$ polyhedra. Ideally the C site is at the Wyckoff 16*c* position (¼, ¼, 0) (Yakubovich et al. 2005), coordinated by six O2 positions at a Wyckoff 96*g* position. The O2 position is therefore only half-occupied. In practice we find that the C site is shifted to a 32*e* position by ($\frac{1}{4} - z$, $\frac{1}{4} - z$, z); the O2 site remains half-occupied, but now the C site is half-occupied as well to prevent unrealistically short distances between adjacent C sites. The CO_3 group orientations in sakhaite are therefore completely disordered.

While initial refinements of the synthetic sakhaite structure by Chichagov et al. (1974) and a natural sakhaite structure by Yakubovich et al. (1978) indicated a space group of $F4_132$ for synthetic sakhaite, all cubic structures in the current study refined in $Fd\bar{3}m$. Space group $F4_132$ is a subgroup of $Fd\bar{3}m$ of index 2; $Fd\bar{3}m$ is obtained from $F4_132$ by the addition of a $\bar{4}$ axis along the crystal axes. No sites are split in the sakhaite structure in lowering the symmetry from $Fd\bar{3}m$ to $F4_132$, so the difference is not in the chemical ordering of any one specific site in the

structure. Yakubovich et al. (2005) suggested that the assignment of $F4_132$ to natural sakhaite was most likely erroneous, although evidence for the synthetic material being acentric seems unambiguous, based on extinction of the reflections 00ℓ (0k0, h00) with $\ell \neq 4n$. If there is a true difference in symmetry between natural and synthetic sakhaite, it seems likely that it is due to an averaging over many minor chemical substitutions and other defects present in natural materials that are absent in synthetic materials with more rigorously controlled environments of formation.

In harkerite, an ordered substitution as in Equation 2 changes the crystal symmetry from cubic ($Fd\bar{3}m$) to rhombohedral ($R\bar{3}m$). Alternating layers of large cavities containing $(HCl,H_2O,\square)(BO_3)_4$ and $Al(SiO_4)_4$ groups are arranged normal to the rhombohedral **c** axis (Fig. 3). The *c* dimension of the rhombohedral unit cell corresponds to twice the body diagonal of the cubic unit cell of sakhaite, thus $c_{\text{harkerite}} \approx 2\sqrt{3}a_{\text{sakhaite}}$ and $a_{\text{harkerite}} \approx a_{\text{sakhaite}}/\sqrt{2}$. There is also some ordering of the CO_3 groups. Two of the three crystallographically distinct CO_3 groups have completely disordered orientations, as in sakhaite; the third, in a layer separating the borate and silicate layers, has an ordered orientation.

Compositions

The 13 single crystal compositions range from sakhaite to harkerite endmembers. The 70 microprobe analyses show that the samples analyzed fall into four categories, which are color-coded in Figures 4-6 and 10: HS12, 14, and 15 are near-endmember sakhaite, with approximately 0 to 3.2 Si sites pfu (blue points); HS10 is the sakhaite-like mineral from Tsumeb, Namibia (Dunn et al. 1990), with 3.8 to 6.1 Si sites pfu (green points); HS1 is an intermediate sakhaite (yellow points), with 5.8 to 8.6 Si sites pfu; and HS11 from Camas Malag (Giuseppetti

et al. 1977) is near-endmember harkerite, with 12.2 to 14.0 Si sites pfu (red points). Ideal endmember harkerite contains 16 Si^{4+} pfu.

Figure 4A shows the variance of measured B and Si contents, with the solid line representing the ideal B + Si = 32 (Eq. 6). All points fall well below the line. The ratio of measured to calculated boron, B/B*, is shown versus calculated boron, B*, in Figure 4B. The spread in measured B appears to increase with the expected amount of B, that is, it decreases with increasing Si. Crystal-structure refinements do not indicate significant vacancies at Si or B sites, nor is there a variation in the O-O edge length of the trigonal B site, consistent with substitution of C (or another cation different in radius to B) for B. This suggests that the B site actually is fully occupied by B, and that B is not being well determined by EMPA. This is likely due to differences in the coordination of B and surrounding matrix between sakhaite-harkerite and the B standard, danburite.

Figure 5 shows the variance of Al on Si content. The solid line shows the Si:Al ratio of 4:1 expected for the ideal $Al(SiO_4)_4$ pentamer. Points for the sakhaite-like mineral and near-endmember harkerite are close to this ideal line; the harkerite points fall slightly below the line, suggesting an excess of Si like that observed by Grew et al. (1999). Points for near-endmember sakhaite, however, fall consistently above the 4:1 line, closer to a Si:Al ratio of 4:1.5 (dashed line in Fig. 5B). This suggests a substitution for Si at the tetrahedral sites; assuming that Al only substitutes for Si, this corresponds to an average aluminosilicate pentamer similar to $Al[(Si_{0.9}Al_{0.1})O_4]_4$. Points for sakhaite intermediate in Si content plot between the two lines.

The interstitial HCl/H_2O site in the large cavity is only occupied when the cavity is surrounded by four BO_3 triangles, since the AlO_4 tetrahedron occupies the same space when the aluminosilicate pentamer is present. The amount of Cl measured pfu should therefore decrease

with increasing Si content, and be less than 1/4 the total occupancy of the B site; in terms of Equations 1 and 4, $n \leq 8 - y$. Figure 6 shows that Cl and Si do indeed have an inverse relationship in most sakhaites and harkerites. For all samples except HS10, the fraction Cl / (¼ B) = n / (8 – y) is between 0.38 and 0.69. The sakhaite-like mineral HS10 (green points), however, is unique in containing almost no Cl (less than 0.25 wt%), and Figure 6 shows that what Cl it does possess is not tied to the Si content. Structure refinements do show that the interstitial site is occupied (see below), so the site must be dominated by H_2O instead.

Sample HS-10 is the same sakhaite-like mineral studied by Dunn et al. (1990) who reported 15.9 wt% B_2O_3 by wet chemistry, well above our EMPA values and somewhat below our calculated values. Dunn et al. (1990) also reported 12.6 wt% CO_2 by wet chemistry, in agreement with our calculated values, and 4.8 wt% H_2O, much higher than our calculated values of 0.21-0.54 wt%. Our EMPA analysis of HS-10 showed significant substitution of Ca by the heavier cations Pb^{2+} (0.39-0.52 atoms pfu, apfu), Sr^{2+} (0.43-0.77 apfu), and rare earth elements (REEs) La^{3+}, Ce^{3+}, and Nd^{3+} (0.06-0.20 apfu total), not observed in other sakhaite compositions.

Structure refinement

Stable crystal-structure refinements were derived from X-ray diffraction data for 14 single crystals: HS1-A, HS1-B, HS1-C, HS1-D, HS2-A, HS10-A, HS10-C, HS11-A, HS11-B, HS14-A, HS14-B, HS15-A, HS15-B, and HS18-A; $R1$ values ranged from 0.0296 to 0.0706. For those refinements with the lowest $R1$ for each category of sakhaite-harkerite − HS15-A and HS14-B (near-end member sakhaites), HS10-A (sakhaite-like mineral), HS1-A (intermediate sakhaite), and HS11-A (near-endmember harkerite) − the refinement parameters, coordinates, and thermal displacement parameters are given in Tables 6, 7, and 8. The crystal structures of samples HS11-

A and HS11-B were best fit with the rhombohedral space group $R\bar{3}m$, while the rest were best fit with the cubic space group $Fd\bar{3}m$. The generally high $R1$ values are due to the large amount of structural disorder in the sakhaite-harkerite series.

During refinement the population of the Al site in the cubic structures was set to exactly 1/4 of the Si site and that of the O3 site (which coordinates the Al site) was set equal to that of the T^{Si} site. In refinements of the HS2-A, HS10-C, HS11-A, HS11-B, and HS15-B crystals the population of (each) B site and its corresponding Si site were constrained to have a total occupancy of 1, while B and Si were allowed to vary independently in the remaining crystals.

All structures except HS14-A and HS14-B have both B and Si sites. In HS14-A and HS14-B, which are near-endmember sakhaites, the Si and Al content in the crystal was too low to refine Si or Al sites. In the near-endmember harkerites HS11-A and HS11-B, the majority Si and B sites were ordered, leading to rhombohedral symmetry. However, the ordering was not perfect. A small number of borate groups (the B1A and B2A sites) occurred in the aluminosilicate layer (occupied by Si1, Si2, and Al sites), while a small number of aluminosilicate groups (the Si1A, Si2A, and AlA sites) occurred in the borate layer. These correspond to ordering defects in the crystal where (B1A, B2A) are occupied instead of (Si1, Si2, Al), or where (Si1A, Si2A, AlA) are occupied instead of (B1, B2). These minority sites account for 5% of total Si and 12% of total B in HS11-A, and 10% of total Si and 19% of total B in HS11-B. That there is approximately twice the fraction of minority B as minority Si in both structures suggest that these are truly disordered sites, as opposed to a second uniform component with opposite ordering to the majority.

Selected bond lengths are given in Table 9. No splitting of the O1 site, which coordinates the Y/Mg site and forms the triangular base of the B/Si coordination polyhedra, was observed. Yakubovitch et al. (2005) reported such a splitting related to replacement of BO_3 triangles by Si

tetrahedra. Instead there is an increase in the O-O distance or side length of the BO_3 triangles with increasing Si content (Fig. 7A, B) as the average position of the O1 site (or equivalent in rhombohedral harkerite) shifts to accommodate the larger Si^{4+} cation. In HS11-A, where Si and B are ordered, O-O side lengths at the T^B sites are consistent with pure B occupation, while basal O-O side lengths at the T^{Si} sites are consistent with pure Si occupation (or mixed Si/Al occupation). Figure 7C shows the mean bond length at the T^{Si} sites for those structures where they could be refined, showing an increase of the bond length with refined T^{Si} occupation. This is certainly in part because as the fraction of Si sites increases, the mean O1 position becomes closer to the local position of a basal O in an SiO_4 tetrahedron, and so the mean T^{Si}–O distance is closer to the preferred Si-O bond length. Conversely, as the Si fraction decreases, the mean O1 position becomes closer to the local position of an O atom in a BO_3 triangle with its shorter O-O sides, and so the mean T^{Si}-O distance is closer to the distance between the T^{Si} site position and the boron-bonded O, which is shorter than the preferred Si-O bond length. However, a second possibility is that in B-rich compositions, the T^{Si} site may be partly occupied by tetrahedral B, so that the mean T^{Si}-O distance is a weighted average of both Si-O and tetrahedral B-O bond lengths. If the B, Si, and O3 site occupations are not linked in a structure refinement, this would lead to an under-populated T^{Si} site if the site was only fit using Si, so that $T^B + T^{Si} < 32$ and $O3 < T^{Si}$. In practice this is difficult to detect, because it is usually necessary to set the O3 and T^{Si} site occupations equal and/or $T^{Si} + T^B = 32$ to converge the structure. Alternatively, tetrahedral B could be detected using infrared spectroscopic methods.

Bond lengths in the minority B and Si sites in harkerite are quite irregular, partly due to their low occupation and high thermal parameters. The Si1A and Si2A tetrahedral sites, which

occur in the otherwise-ordered borate layers, are good potential candidates to actually be tetrahedral B instead of Si, due to their low average bond lengths.

Chemical formulae for seven single crystals with both X-ray structure refinements (SREF) and EMPA data are given in Table 10. For HS10, the EMPA formula is the median of 22 analyses of four crystals (HS10-1, -2, -3, and -4), and the SREF formula is the mean of results for crystals HS10-A and HS10-C. Note that the SREF formulae will not be charge balanced; the net formula charge is between –1.9 and –3.8, while the error in the calculated charge is of a similar magnitude. Except for HS10, the EMPA formulae have a net charge between +0.04 and –0.05, because the atomic proportions are medians multiple analysed points over the crystal, as in table 3; the HS10 formula is a median over different crystals, and so has net charge of –2.4 with error 2.7. There is generally good agreement between the SREF and EMPA formulae. Agreement between SREF and EMPA for the Cl/interstitial site is fair except for HS10-A, which is discussed below. The occupancy of the interstitial site refined by SREF is consistently higher for near-endmember and intermediate sakhaite samples HS1-D, HS14-A, HS14-B, and HS15-A. This may suggest that both HCl and H_2O are present at the interstitial site in most sakhaites, with HCl dominating. The near-endmember harkerite HS11-A and HS11-B crystals show the opposite trend, with the EMPA occupancy higher than the refined occupancy; the reason for this is unknown.

From the EMPA data, HS-10 has a very low Cl content compared to other sakhaites, only around 0.3 apfu. However, the interstitial site in HS10-A has a refined occupancy of 2.0(2) apfu Cl and for HS10-B, the refined occupancy is 3.6(7) apfu Cl. The interstitial site in the sakhaite-like mineral must therefore be dominated by H_2O. If the sakhaite-like mineral has the interstitial

site dominated by H_2O while HCl dominates in other sakhaites, it may qualify as a distinct mineral.

Figure 8 shows a distinct linear dependence of the cubic unit-cell parameter *a* (or equivalent for rhombohedral near-endmember harkerite) with the refined Si content. The unit-cell dimension increases as the Si content increases, with a fitted trend of

$$a = 0.19\frac{\mathrm{Si}}{16} + 14.63\ \text{Å} \quad (R^2 = 0.992) \tag{6}$$

As the Si content increases, the structure expands to accommodate more $Al(SiO_4)_4$ pentamers. The sakhaite-like mineral HS10 is the exception to this trend, having much higher unit-cell parameters than predicted by Equation 6 based on Si content. The expansion of the unit cell in comparison to other sakhaites with comparable Si content may be due to substitution of Ca by Pb, Sr, or other heavy cations.

The rhombohedral harkerite structure with the lowest Si content is HS11-B, with 14.0 Si pfu, while the cubic sakhaite structure with the highest Si content is HS1-C, with 7.7 Si pfu. The structural transition from cubic to rhombohedral symmetry lies somewhere in between. The presence of minority Si in the borate layer and B sites in the aluminosilicate layers of rhombohedral harkerite suggests this transition may be gradual. Endmember harkerite is defined with Si = B = 16; equal proportions allows perfect ordering, which leads to rhombohedral symmetry. Although a harkerite composition with Si > B has not been observed, presumably at a high enough Si content the structure would revert back to cubic. There is no a priori reason that a composition with equal proportions of Si and B must be ordered; such a composition could be disordered, with borate and aluminosilicate groups distributed randomly rather than in layers, and therefore maintain cubic symmetry. Under the current definition of harkerite, it is not clear if this hypothetical composition would be "cubic harkerite" or "high-silicate sakhaite".

Coordination geometry of the C and X sites

The X site in sakhaite and harkerite is usually dominated by Ca. In sakhaite, it is coordinated by the O1 and O2 oxygen sites; O1 also coordinates the octahedral Y (Mg), T^B, and T^{Si} sites while O2 coordinates the C site. In most sakhaite compositions, X is coordinated by six O1 and six O2 each (Table 9A), and since the O2 site is half occupied, the average X site is nine-coordinated. However Table 9B shows that in the sakhaite-like material HS10, X is coordinated by four O1 and eight O2, and so on average is only eight-coordinated. Why the difference? The local symmetry of the C site, and whether the orientation of the CO_3 triangle is ordered or disordered, affects the coordination geometry of the X site.

In the near-endmember and intermediate sakhaites, represented here by HS1-A, the C site (Fig. 9A) is offset from space group $Fd\bar{3}m$'s Wyckoff 16*c* position at (1/4, 1/4, 0) to 32*e* at (1/4 – *x*, 1/4 – *x*, *x*). If the C and O2 sites are fully occupied, there are two parallel CO_3 triangles, oriented in opposite directions, separated by 0.71(2) Å. The two triangles cannot be present simultaneously, therefore the C and O2 sites must be half occupied. The orientation of the CO_3 triangle is thus disordered, with 50% pointing in either direction. The distance from a C site to the next nearest set of O2 sites is 1.470(8) Å; the C site could thus potentially accommodate a slightly larger cation, such as B, in trigonal pyramidal coordination.

The local environment of the X site in HS1-A is shown in Figure 9B. The X site is coordinated by six O1 and six O2 sites. The O1 sites are all fully occupied and arranged in a 1 + 4 + 1 configuration around the X site. The O2 sites are arranged in groups of 3 (O2a, O2b, and O2c in Fig. 9B) on either side of the X site. Here the X polyhedra shares either an edge (O2a-O2b) or a corner (O2c) with a CO_3 triangle, depending on the orientations of the surrounding

triangles. With randomly oriented CO_3 triangles, 25% of the X sites are eight-coordinated, 50% are nine-coordinated, and 25% are 10-coordinated, for an average coordination number of nine.

In the sakhaite-like material, represented here by HS10-A, there are also closely spaced, paired C sites (Fig. 10A), but an additional displacement of the O2 site from Wyckoff 96*g* to 192*i* introduces additional disorder, doubling the O2 site, which now must be only one-quarter occupied. The CO_3 triangles may now point in either orientation, as well as being on either side of the 16*c* position.

The X site in HS10-A is split into Ca-dominated and Pb/Sr-dominated sites. The X sites (both Ca and Pb) are now adjacent to six fully occupied O1 sites and 12 partially occupied O2 sites (Fig. 10B, C). The O2a, O2b, and O2c sites in Figure 9B become O2a', O2b', O2c' and O2a", O2b", O2c" in Figure 10B. The displacement of the O2 site also causes rotation of the CO_3 triangles with respect to the X polyhedra, moving O2a' and O2b" towards and O2a" and O2b' away from the cation. The consequence is that O2a" and O2b' are no longer at bonding distances [3.266(9) Å] to Ca, and so the Ca polyhedra only share corners (O2c', O2c", O2a', or O2b") with adjacent CO_3 triangles. All Ca polyhedra in HS10-A are therefore eight-coordinated.

The Pb site is shifted from the Ca site by 0.41(8) Å, away from the rectangular face bounded by four O1 atoms (see Fig. 10B, C). This significantly shortens bonds with O2 from 2.38(1) and 2.394(9) Å to 2.17(1) and 2.28(1) Å, but lengthens the four O1 bonds from 2.524(2) Å to 2.81(2) Å. The Pb site also gains bonds of 2.80(2) Å with O3 when the latter site is present [the minimum Ca-O3 distance site is 3.045(2) Å]. Taking into account occupation of the O2 and O3 sites, the mean Pb-O bond length is 2.60 Å, approximately 4% larger than the mean Ca-O bond length. The incorporation of larger cations like Pb^{2+}, Sr^{2+}, and rare earths at the Pb site may be responsible for the rotation of the CO_3 triangles that eliminates edge-sharing.

In near-endmember harkerites such as HS11-A, the C site is split into three positions. The structure contains 12 C1 sites pfu, and 2 sites pfu each of C2 and C3. The C1 site (Fig. 11A) is located at a Wyckoff 18*h* position (point group symmetry *m*) in space group $R\bar{3}m$, coordinated by two O10 and one O11 site. None of these sites are duplicated and all are fully occupied, so the $(C1)O_3$ triangle is ordered with just a single orientation. The C2 site (Fig. 11B) is located at a Wyckoff 3*a* site (symmetry $\bar{3}2/m$) and is coordinated by six O12 sites at 1.273 Å. As in HS10-A, only three O12 sites can be occupied at a time to avoid unrealistically short O-O distances. The O12 sites must be half occupied, and the $(C2)O_3$ triangles will have two possible orientations. The C3 site (Fig. 11C) is located at a Wyckoff 6*c* position (point group 3*m*), and as in HS1-A both C3 and the coordinating O13 sites are half-occupied. Two orientations are possible for the $(C3)O_3$ triangles, separated by 1.04 Å. The C3 site is only 1.78 Å from the closest Cl site, which is a bonding distance for C-Cl [the C-Cl bond length calculated from Shannon and Prewitt (1976) is 1.73 Å; in organic molecules, C-Cl bonds range from 1.63-1.78 Å (Sutton 1958)]. The shortest C-Cl distance in HS1-A is 2.11(3) Å. There is no apparent distortion of the $(C3)O_3$ triangle away from planar, however, which suggests that C-Cl bonding is not significant. It seems likely that the Cl and C sites are populated such that a short C-Cl distance is avoided, which suggests that C-Cl bonding is not significant.

As with the C site, the X (Ca) site is split in the rhombohedral structure. The Ca1-Ca4 sites each contribute 12 sites pfu. They differ in coordination, because they share elements with different CO_3 triangles. The simplest case is the Ca4 site (Fig. 12D), which shares a corner (O10) with two C1 triangles. As the O10 site is always occupied, the Ca4 site is always eight-coordinated. Similarly, Ca3 shares O10-O11 edges with two C1 triangles, and so is always at least 10-coordinated. When the O15 site (grey sphere in Fig. 12C), which coordinates the

minority Si2A and AlA sites, is present, it also is within bonding distance (< 3 Å) of Ca3, and so Ca3 is occasionally 11-coordinated. The Ca1 site (Fig. 12A) shares corners with a C1 triangle (O11) and a C2 triangle (O12) which may be of either possible orientation. The Ca1 polyhedron thus occurs in two mirror-image forms with 50% probability, both of which are eight-coordinated. Finally, the Ca2 site (Fig. 12B) coordination is the most complex, with 13 oxygen sites within bonding distance. The Ca2 site shares an edge (O10-O10) with a C1 triangle and either an edge or a corner with a $(C3)O_3$ triangle, depending on the latter's orientation. Ca2 may also bond to adjacent O14 sites (grey spheres in Fig. 12B), sharing edges (O1-O14) with two Si1A sites and the AlA site of a minority aluminosilicate pentamer. The minimum O14-O15 distance of 2.04 Å is unrealistically short, however, so when Ca2 bonds to the two O14 sites it must only share a corner with the $(C3)O_3$ triangle. In other words, the presence of the minority aluminosilicate pentamer forces the orientation of the $(C3)O_3$ triangle. As a result the Ca2 site is either nine-, 10-, or infrequently 11-coordinated.

For comparison, the X site in the $F4_132$ structure of synthetic sakhaite from Chichagov et al. (1974) is shown in Figure 13. The C site (not shown) in the $F4_132$ structure is missing a mirror through the C site in the $Fd\bar{3}m$ structure that causes the doubling of the coordinating O2 seen in Figures 11 and 12; as a result there is only a single orientation for the CO_3 triangles as opposed to the multiple possible orientations in variations of the $Fd\bar{3}m$ structure. The O2 site is fully occupied. The X site in the $F4_132$ structure shares corners with two CO_3 triangles, and so there is a unique, non-mirror symmetric eight-coordinate polyhedron. The implication is that synthetic sakhaite has ordered CO_3 triangles, lacking in natural sakhaite with non-zero Si content, which leads to the lower space group.

Implications

The harkerite-sakhaite series is unique among minerals both in containing essential carbonate, borate, and silicate groups and as being a solid solution involving clusters of polyhedra instead of single polyhedra or anions. The substitution (☐, HCl, H_2O)$(BO_3)_4$ → $Al_{1+a}Si_{4-a}O^*_{16}$ summarizes this solid solution. In endmember harkerite, 50% of the borate groups are replaced by aluminosilicate groups in an ordered substitution that reduces the space group symmetry from cubic to rhombohedral. The change in symmetry is constrained to lie between 7.7 and 14.0 Si pfu, i.e., not necessarily at the midpoint of 8.0 Si pfu (for $a = 0$) between end member sakhaite and harkerite. Further complications are introduced by partial disordering of aluminosilicate layers and borate layers induced by mixing of borate groups and aluminosilicate groups in individual layers, thereby implying the possibility of a disordered phase with the symmetry of sakhaite and the composition of harkerite. The current definition of harkerite relies on composition only and does not specify whether rhombohedral symmetry is essential to the mineral's identity.

Potential for species diversity is not limited to the substitution (☐, HCl, H_2O)$(BO_3)_4$ → $Al_{1+a}Si_{4-a}O^*_{16}$ and symmetry changes tied to order/disorder. The interstitial site surrounded by borate groups appears to be dominated by HCl when occupied in most sakhaite-harkerite compositions, whereas it contains little HCl in the sakhaite-like mineral from Tsumeb, Namibia (Dunn et al. 1990), in which H_2O appears to be dominant instead. If the interstitial site can be used to distinguish species, the number of potential species increases to 6: two sets of H_2O-, HCl- and ☐-dominant species, of which the "sakhaite-like" mineral would a new H_2O-dominant analogue of sakhaite. The Si-free sakhaite synthesized by Nekrasov and Malinko (1973) contains

1.57 wt% Cl, corresponding to about 2.4 Cl pfu, insufficient to fill 50% of the interstitial site, and thus the Si-free compound could be the synthetic analogue of the "sakhaite-like" mineral.

However, recognizing new species based on occupancy of the interstitial site is premature; this site is one of the least well understood aspects of the sakhaite-harkerite series. Are we dealing with only HCl and H_2O, or could Cl^- and OH^- be playing a role? Our analyses suggest the possible presence of F^- and/or HF as well. Moreover, other questions remain concerning H_2O: Nekrasov and Malinko (1973) reported 3.5 wt%, corresponding to over 10 H_2O pfu. Unless this H_2O determination is greatly in error, the calculated H_2O content exceeds the $4H_2O$ pfu (allowing for 2 Cl pfu in the analysis) available according to the formula for sakhaite. Where could this "excess" H_2O be located in the structure? Given the current interest in microporous materials and practical applications, the sakhaite-harkerite series have potential for detailed experimental studies of various compositions including other cations such as Pb and REE, which are present in the "sakhaite-like" mineral, as well as halogens and H_2O.

ACKNOWLEDGMENTS

The authors thank Mackenzie Parker and Jordan Roberts for help preparing the manuscript, the reviewers, Associate Editor G. Diego Gatta, and the Editor for their comments. We acknowledge the support of the Natural Sciences and Engineering Research Council of Canada (NSERC), funding reference 06434. The following institutions and individuals are thanked for samples: National Museum of Natural History (Smithsonian Institution), Pavel M. Kartashov, and Nikolai N. Pertsev.

REFERENCES CITED

Barbieri, N., Cozzupoli, D., Federico, M., Fornaseri, M., Merlino, S., Orlandi, P., and Tolomeo, L. (1977) Harkerite from the Alban Hills (Italy). Lithos, 10, 133–141.

Bruker (2007) SAINT. Bruker AXS Inc., Madison, Wisconsin.

Chichagov, A.V., Simonov, M.A., and Belov, N.V. (1974) Crystal structure of sakhaite $Ca_3Mg(BO_3)_2CO_3 \cdot xH_2O$. Doklady Akademii Nauk SSR, 218, 576–579.

Creagh, D.C. and Hubbell, J.H. (1992) International Tables for Crystallography, vol. C., p. 200–206. Kluwer Academic Publishers, Boston.

Creagh, D.C. and McAuley, W.J. (1992) International Tables for Crystallography, vol C., p. 219–222. Kluwer Academic Publishers, Boston.

Cromer, D.T. and Waber, J.T. (1974) International Tables for X-ray Crystallography, Vol. IV. The Kynoch Press, Birmingham, England.

Davies, W.O. and Machin, M.P. (1970) Isomorphous replacements in harkerite and the relation of sakhaite to harkerite. Canadian Mineralogist, 10, 689–695.

Dirken, P.J., Kentgens, A.P.M., Nachtegaal, G.H., van der Eerden, A.M.J., and Jansen, J.B.H. (1995) Solid-state MAS NMR study of pentameric aluminosilicate groups with 180° intertetrahedral Al-O-Si angles in zunyite and harkerite. American Mineralogist, 80, 39–45.

Dunn, P.J., Peacor, D.R., Nelen, J.A., Ramik, R.A., and Innes, J. (1990) A sakhaite-like mineral from the Kombat Mine in Namibia. Mineralogical Magazine, 54, 105–108.

Galuskina, I.O., Kadiyski, M., Armbruster, T., Galuskin, E.V., Pertsev, N.N., Dzierzanowski, P., and Wrzalik, R. (2008) A new natural phase in the system Mg_2SiO_4–Mg_2BO_3F–

$Mg_2BO_3(OH)$: Composition, paragenesis and structure of OH-dominant pertsevite. European Journal of Mineralogy, 20, 951–964.

Giuseppetti, G., Mazzi, F., and Tadini, C. (1977) The crystal structure of harkerite. American Mineralogist 62, 263–272.

Grew, E. S. (1996) Borosilicates (exclusive of tourmaline) and boron in rock-forming minerals in metamorphic environments. In E.S. Grew and L.M. Anovitz, Eds., Boron: Mineralogy, Petrology and Geochemistry, 33, p. 387-502. Reviews in Mineralogy, Mineralogical Society of America, Chantilly, Virginia.

Grew, E.S., Yates, M.G., Adams, P.M., Kirkby, R., and Wiedenbeck, M. (1999) Harkerite and associated minerals in marble and skarn from Crestmore Quarry, Riverside County, California, and Cascade Slide, Adirondack Mountains, New York. Canadian Mineralogist, 37, 277–296.

Ibers, J.A. and Hamilton, W.C. (1964) Dispersion corrections and crystal structure refinements. Acta Crystallographica, 17, 781–782.

Machin, M.P. and Miehe, G. (1976) $[Al(SiO_4)_4]_{13}$– tetrahedral pentamers in harkerite. Neues Jahrbuch für Mineralogie Monatshefte, 5, 228–232.

Malinko, S.V. and Kuznetsova, N.N. (1973) A new find of sakhaite. Zapiski Vsesoyuznogo Mineralogicheskogo Obshchestva, 102(2), 164–170.

McGee, J.J. and Anovitz, L.M. (1996): Electron probe microanalysis of geologic materials for boron. In E.S. Grew and L.M. Anovitz, Eds., Boron: Mineralogy, Petrology and Geochemistry, 33, p. 771-788. Reviews in Mineralogy, Mineralogical Society of America, Chantilly, Virginia.

Merlet, C. (1994) An accurate computer correction program for quantitative electron-probe microanalysis. Microchimica Acta, 114, 363–376.

Mihajlović, T., Lengauer, C.L., Ntaflos, T., Kolitsch, U., and Tillmanns, E. (2004) Two new minerals, rondorfite, $Ca_8Mg[SiO_4]_4Cl_2$, and almarudite, $K(\square,Na)_2(Mn,Fe,Mg)_2(Be,Al)_3[Si_{12}O_{30}]$, and a study of iron-rich wadalite, $Ca_{12}[(Al_8Si_4Fe_2)O_{32}]Cl_6$, from the Bellerberg (Bellberg) volcano, Eifel, Germany. Neues Jahrbuch für Mineralogie Abhandlungen, 179, 265–294.

Momma, K. and Izumi, F. (2011) VESTA 3 for three-dimensional visualization of crystal, volumetric and morphology data. Journal of Applied Crystallography, 44, 1272–1276.

Nekrasov, I.Ya. and Malinko, S.V. (1973) Experimental study of the conditions of formation of sakhaite. Doklady Akademii Nauk SSSR, 210, 1427–1430.

Ostrovskaya, I.V. (1969) Crystal structure of harkerite and sakhaite. Trudy Mineralogicheskogo Muzeya Akademii Nauk SSR, 19, 197–201.

Ostrovskaya, I.V., Pertsev, N.N., and Nikitina, I.B. (1966) Sakhaite, a new carbonatoborate of calcium and magnesium. Zapiski Vsesoyuznogo Mineralogicheskogo Obshchestva, 95, 193–202.

Shannon, R.D. (1976) Revised effective ionic radii and systematic studies of interatomic distances in halides and chalcogenides. Acta Crystallographica, A32, 751–767.

Sheldrick, G.M. (1996) SADABS. University of Göttingen, Germany.

Sheldrick, G.M. (2008) A short history of SHELX. Acta Crystallographica, A64, 112–122.

Sutton, L.E. (1958) Tables of Interatomic Distances and Configuration in Molecules and Ions, The Chemical Society, London.

Tilley, C.E. (1951) The zoned contact-skarns of the Broadford area, Skye: A study of boron-fluorine metasomatism on dolomites. Mineralogical Magazine, 29, 640–667.

Yakubovich, O.V., Yegorov-Tismenko, Y.K., Simonov, M.A., and Belov, N.V. (1978) The crystal structure of natural sakhaite $Ca_3Mg[BO_3]_2[CO_3]\cdot 0.36H_2O$. Doklady Akademii Nauk SSR, 239, 1103–1106.

Yakubovich, O.V., Still, I.M., Gavrilenko, P.G., and Urusov, V.S. (2005) Crystal structure of sakhaite from the Solongo deposit in connection with the crystallochemical interpretation of the sakhaite-harkerite mineral series. Crystallography Reports, 50, 194-202.

FIGURE CAPTIONS

FIGURE 1. The crystal structure of sakhaite. (A) A single layer of the CaO_{9-11} polyhedral framework, showing cavities. (B) Two layers of the framework, showing adjacent MgO_6 octahedra. (C) The endmember sakhaite structure with MgO_6 octahedra hidden, showing positions of the BO_3 triangles, CO_3 triangles, and HCl/H_2O at the interstitial sites.

FIGURE 2. The substitution in the sakhaite-harkerite series involves replacement of four BO_3 triangles (A) with a pentamer consisting of four SiO_4 tetrahedra surrounding an AlO_4 tetrahedron (B). The cavity surrounded by the BO_3 groups contains HCl or H_2O (dotted circle) displaced from the center of the cavity.

FIGURE 3. Borate and aluminosilicate layers in harkerite. Only the interstitial sites (green spheres) in the midst of the borate triangles and AlO_4 tetrahedra (pink tetrahedra) are shown for clarity.

FIGURE 4. (A) B vs. Si content in atoms per formula unit (apfu). The solid line indicates the ideal B + Si = 32 apfu. (B) Ratio of measured boron (B) to calculated boron (B*) vs. calculated boron (B*).

FIGURE 5. Al vs. Si content in apfu. The solid line indicates the ideal Si:Al ratio of 4:1, the dashed line represents a ratio of 4:1.5.

FIGURE 6. Cl vs. Si content in apfu.

FIGURE 7. O-O edge distance in T^B triangles / T^{Si} tetrahedra versus Si (apfu) determined from (A) EMPA and (B) structure refinement (SREF). (C) Average T^{Si}-O distance versus Si (apfu) from structure refinement.

FIGURE 8. Cubic *a* unit-cell parameter vs. refined Si for all sakhaite-harkerite structures. For the rhombohedral cells, an equivalent a_{cubic} is calculated as the mean of $\sqrt{2}a$ and $\frac{1}{2\sqrt{3}}c$.

FIGURE 9. (A) C site and (B) X (Ca) site in HS1-A. Brown spheres are C, blue-green sphere is Ca, red spheres are O1, magenta spheres are O2.

FIGURE 10. (A) C site, (B) X (Ca) site, and (C) X (Pb) site in HS10-A. Brown spheres are C, blue-green sphere is Ca, dark grey sphere is O3, red spheres are O1, magenta spheres are O2, purple spheres are O3.

FIGURE 11. C sites in HS11-A. Brown spheres are C; cyan spheres are oxygen coordinating site C1; magenta spheres are oxygen coordinating C2; yellow spheres are oxygen coordinating C3; green spheres are Cl. (A) C1, (B) C2, (C) C3.

FIGURE 12. The X (Ca) sites in HS11-A. The blue-green spheres are Ca; cyan spheres are oxygen coordinating site C1; magenta spheres are oxygen coordinating C2; yellow spheres are

oxygen coordinating C3; red spheres are oxygen shared with Mg, B, and Si sites; and grey spheres are oxygen shared with Si and Al sites. (A) Ca1, (B) Ca2, (C) Ca3, (D) Ca4.

FIGURE 13. The X (Ca) site in the synthetic sakhaite composition of Chichagov et al. (1974). Blue-green sphere is Ca, red spheres are O1, magenta spheres are O2.

This is a preprint, the final version is subject to change, of the American Mineralogist (MSA)
Cite as Authors (Year) Title. American Mineralogist, in press.
DOI: https://doi.org/10.2138/am-2018-6563

(A)

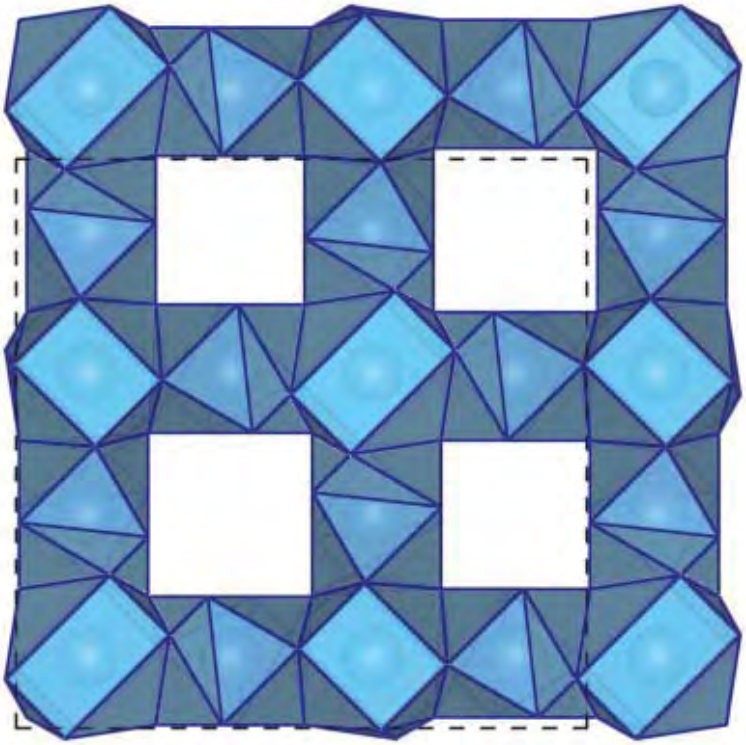

(B)

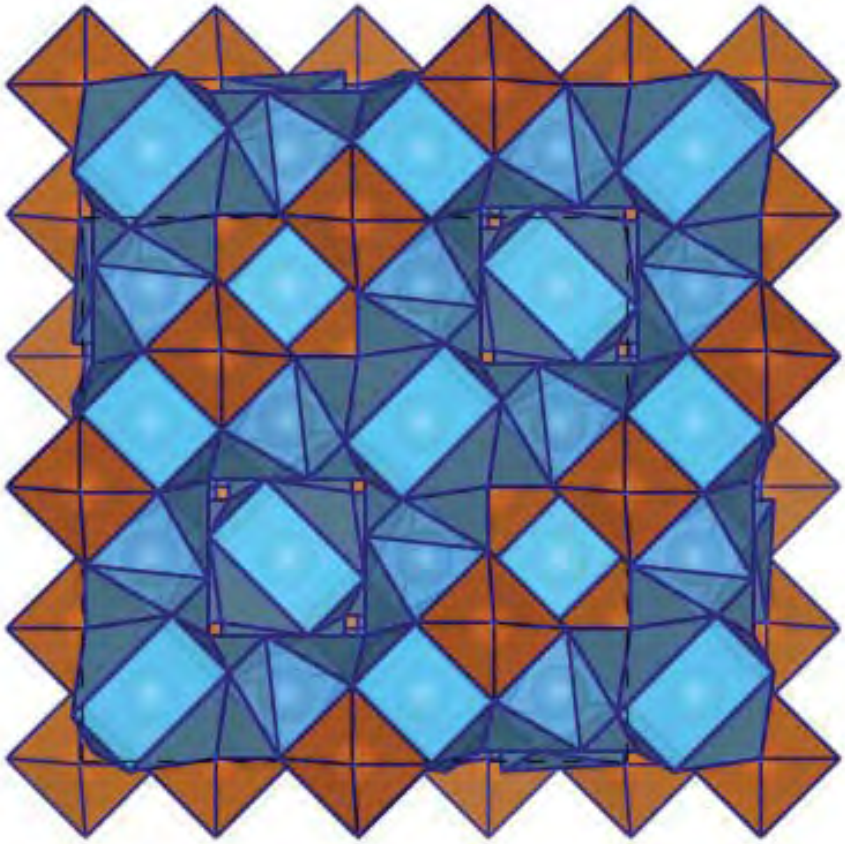

This is a preprint, the final version is subject to change, of the American Mineralogist (MSA)
Cite as Authors (Year) Title. American Mineralogist, in press.
DOI: https://doi.org/10.2138/am-2018-6563

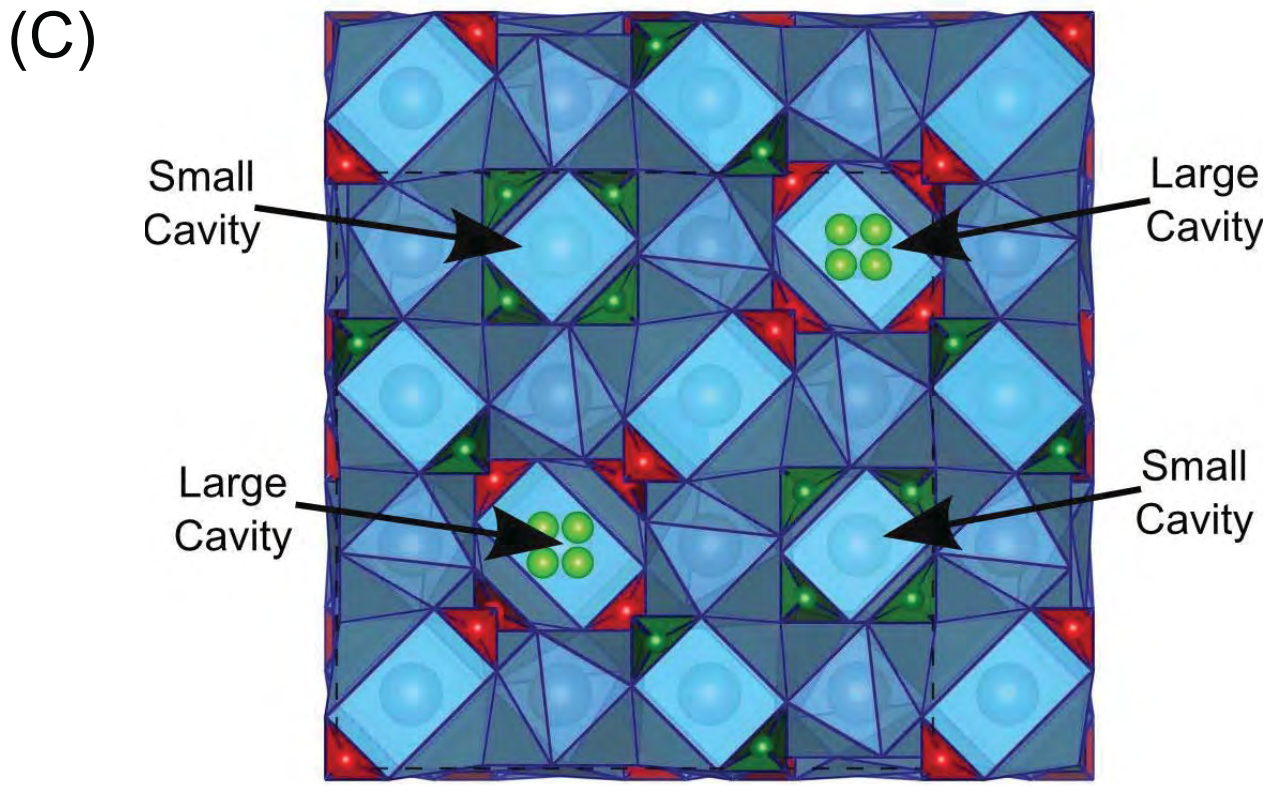

FIG. 1.

This is a preprint, the final version is subject to change, of the American Mineralogist (MSA)
Cite as Authors (Year) Title. American Mineralogist, in press.
DOI: https://doi.org/10.2138/am-2018-6563

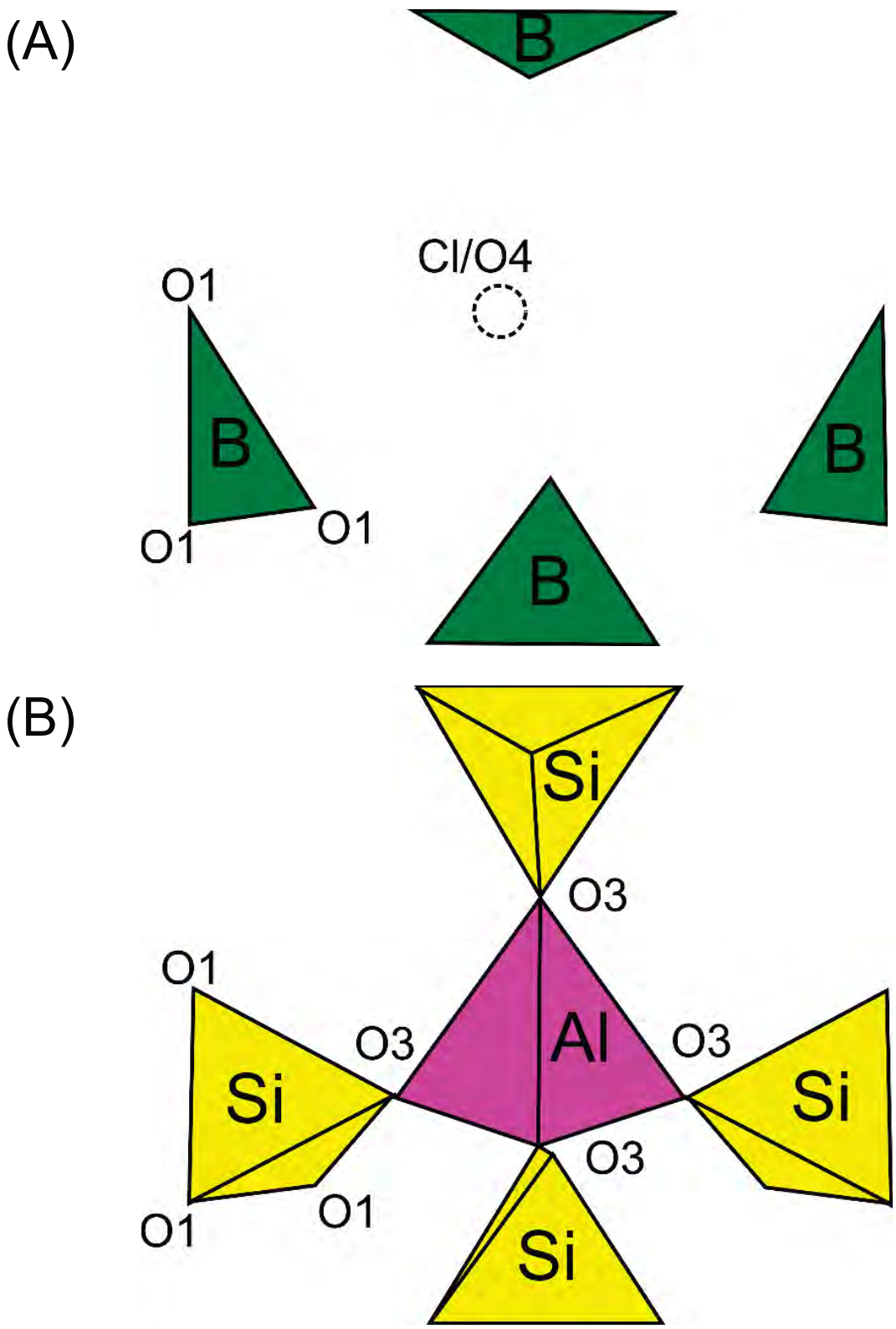

FIG. 2.

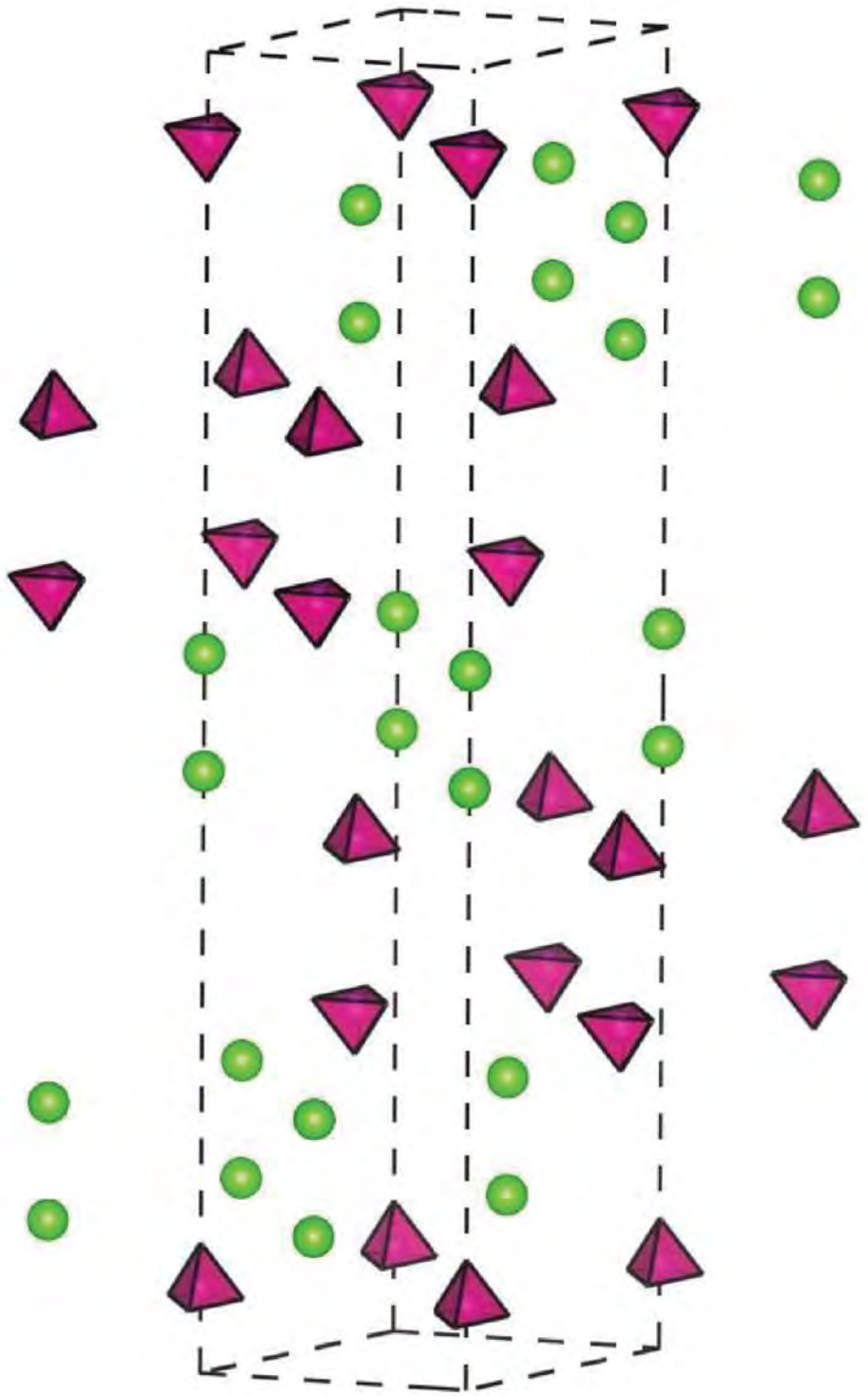

FIG. 3.

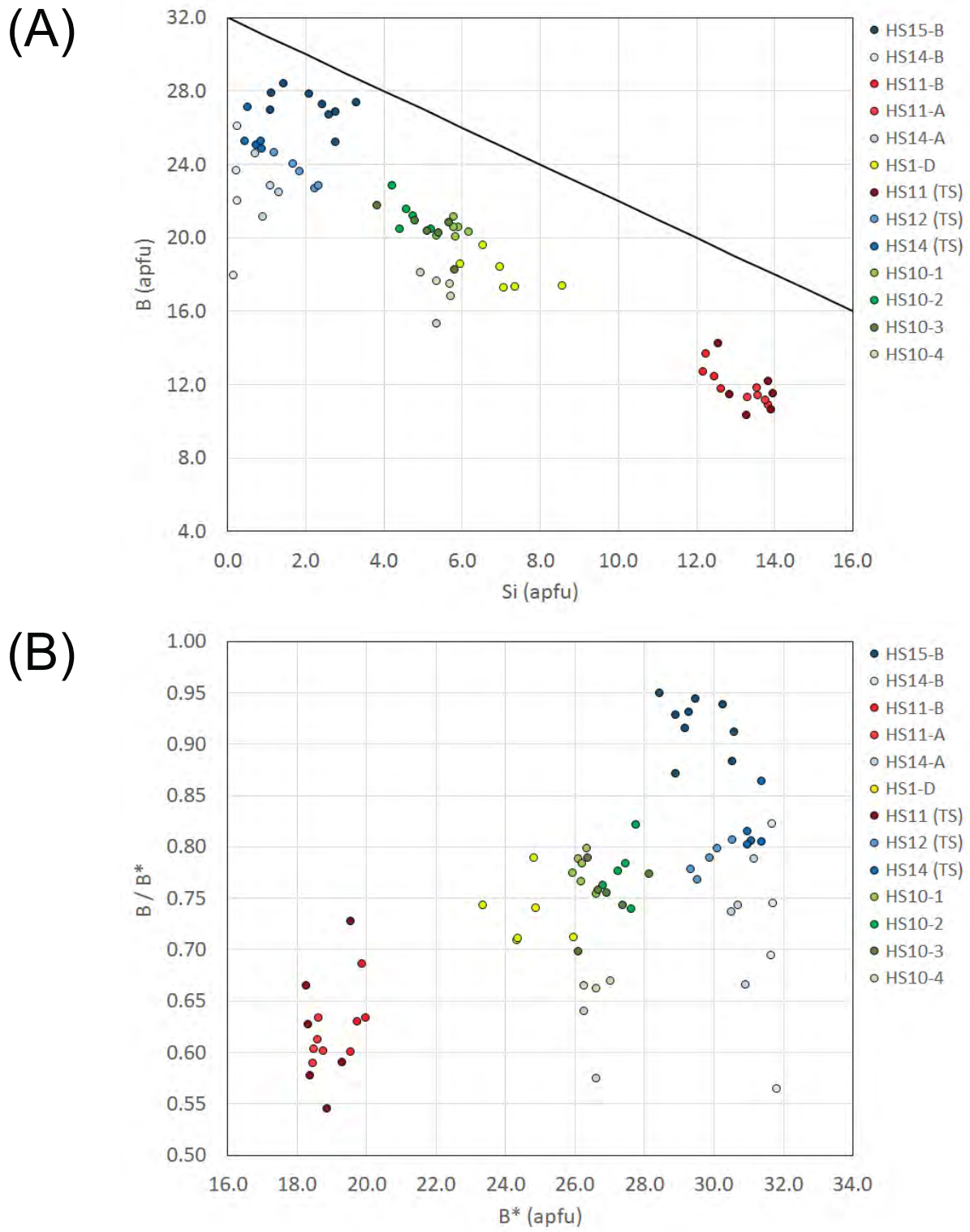
(A)
B (apfu)
Si (apfu)
32.0
28.0
24.0
20.0
16.0
12.0
8.0
4.0
0.0
2.0
4.0
6.0
8.0
10.0
12.0
14.0
16.0
HS15-B
HS14-B
HS11-B
HS11-A
HS14-A
HS1-D
HS11 (TS)
HS12 (TS)
HS14 (TS)
HS10-1
HS10-2
HS10-3
HS10-4
(B)
B / B*
B* (apfu)
1.00
0.95
0.90
0.85
0.80
0.75
0.70
0.65
0.60
0.55
0.50
16.0
18.0
20.0
22.0
24.0
26.0
28.0
30.0
32.0
34.0
HS15-B
HS14-B
HS11-B
HS11-A
HS14-A
HS1-D
HS11 (TS)
HS12 (TS)
HS14 (TS)
HS10-1
HS10-2
HS10-3
HS10-4

FIG. 4.

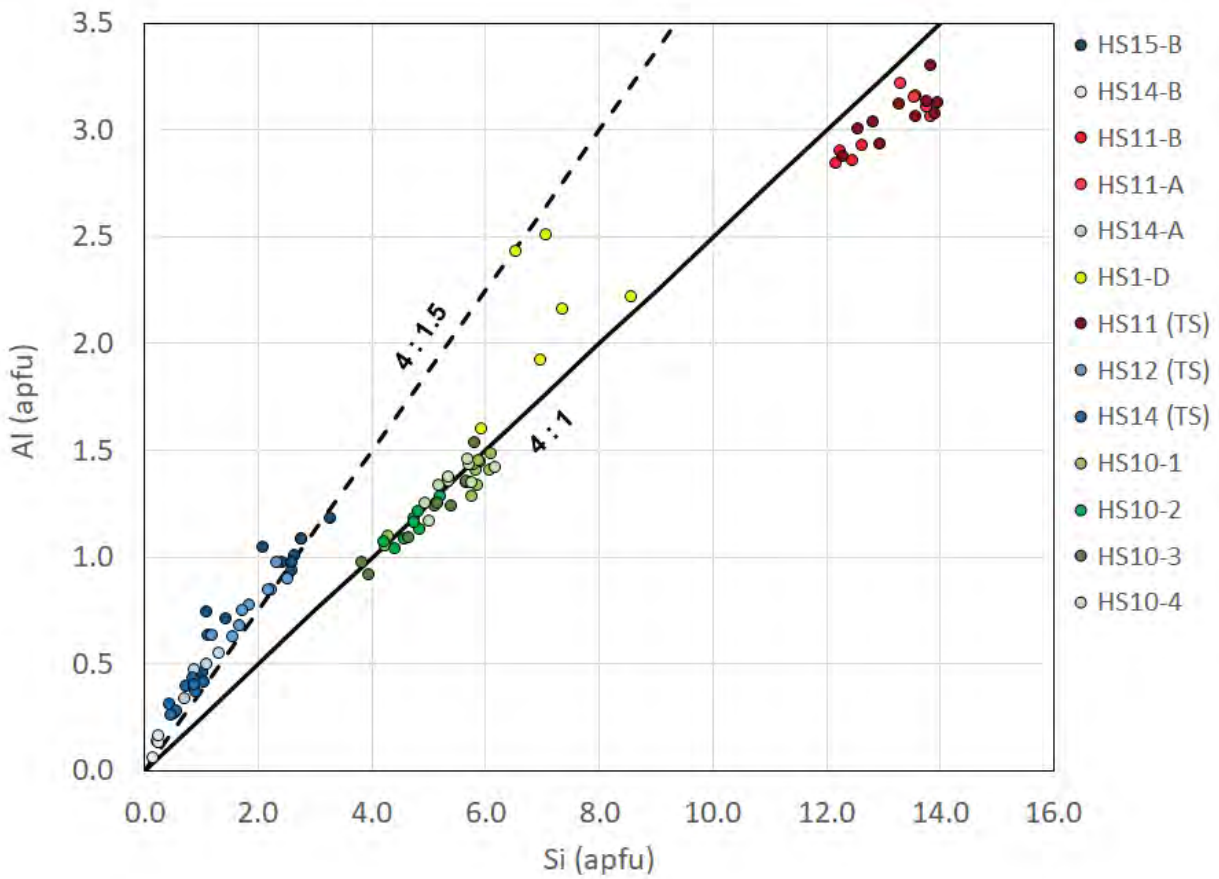
3.5
3.0
2.5
2.0
1.5
1.0
0.5
0.0
Al (apfu)
0.0
2.0
4.0
6.0
8.0
10.0
12.0
14.0
16.0
Si (apfu)
4 : 1.5
4 : 1
HS15-B
HS14-B
HS11-B
HS11-A
HS14-A
HS1-D
HS11 (TS)
HS12 (TS)
HS14 (TS)
HS10-1
HS10-2
HS10-3
HS10-4

FIG. 5.

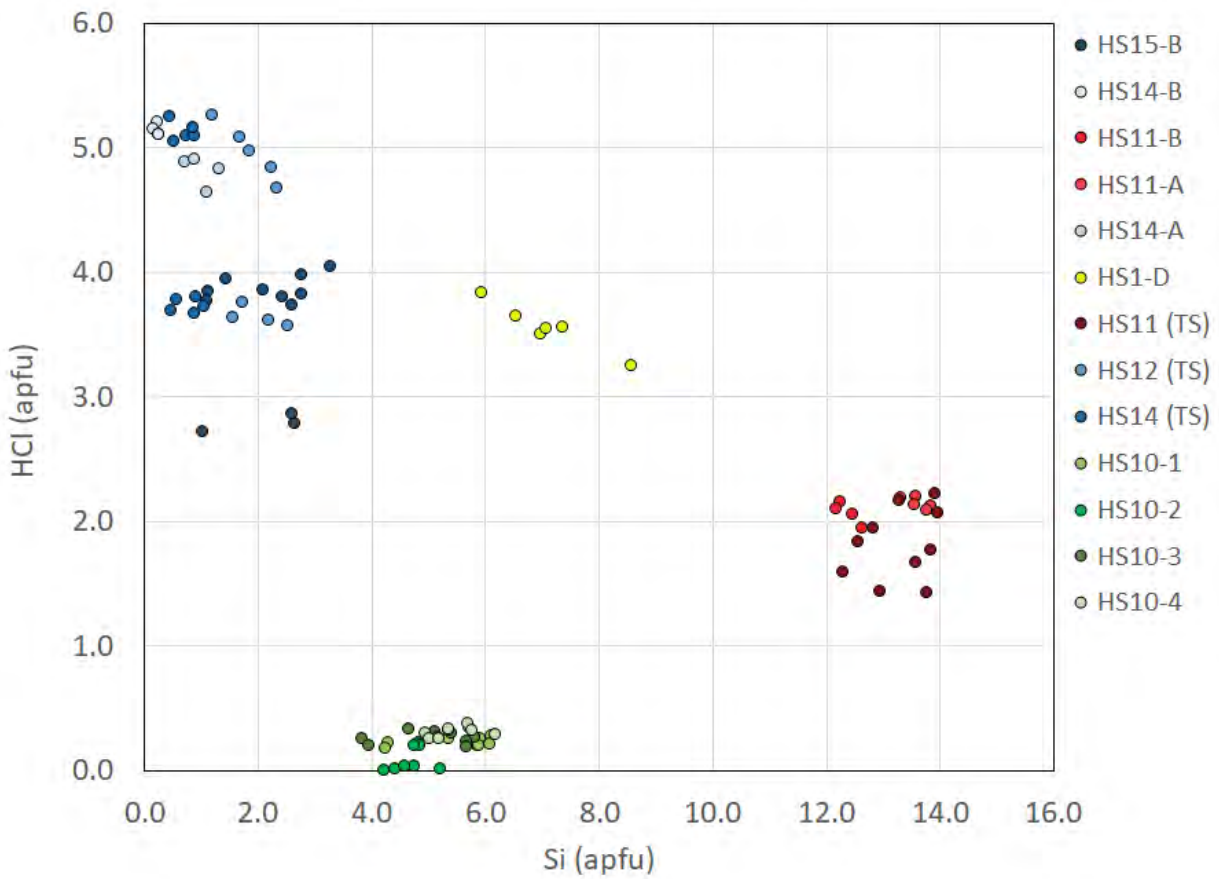
6.0
5.0
4.0
3.0
2.0
1.0
0.0
HCl (apfu)
0.0
2.0
4.0
6.0
8.0
10.0
12.0
14.0
16.0
Si (apfu)
HS15-B
HS14-B
HS11-B
HS11-A
HS14-A
HS1-D
HS11 (TS)
HS12 (TS)
HS14 (TS)
HS10-1
HS10-2
HS10-3
HS10-4

FIG. 6.

(A)

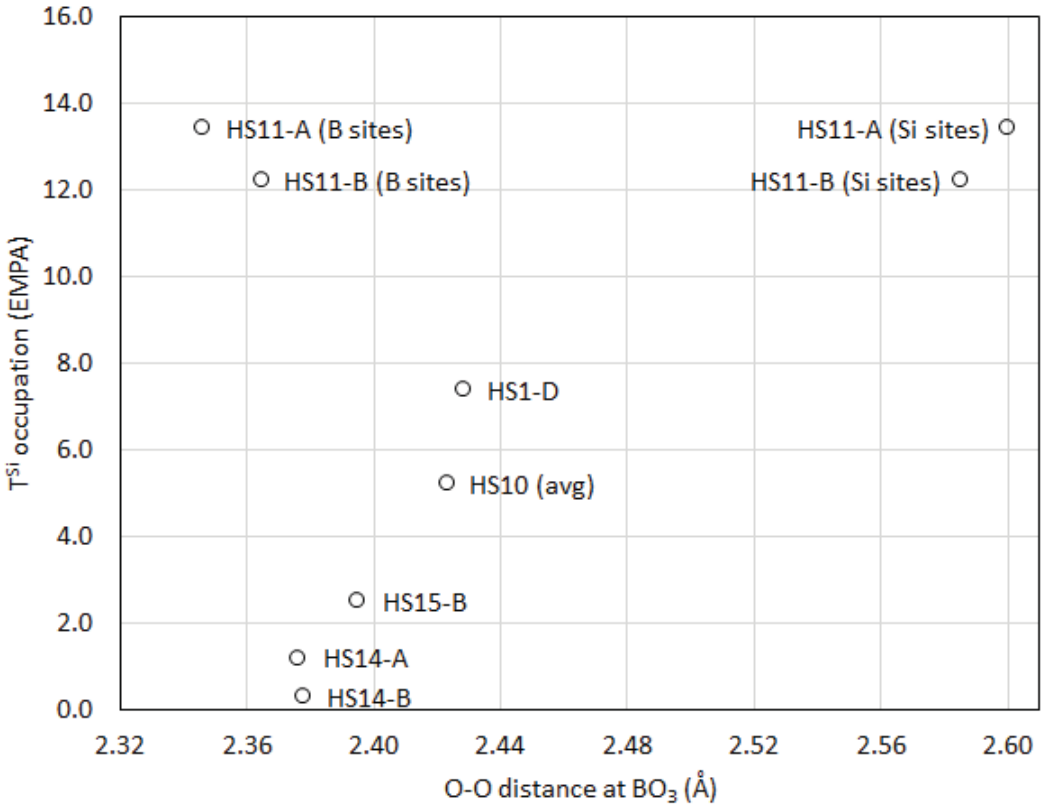
16.0
14.0
12.0
10.0
8.0
6.0
4.0
2.0
0.0
T^{Si} occupation (EMPA)
HS11-A (B sites)
HS11-B (B sites)
HS11-A (Si sites)
HS11-B (Si sites)
HS1-D
HS10 (avg)
HS15-B
HS14-A
HS14-B
2.32
2.36
2.40
2.44
2.48
2.52
2.56
2.60
O-O distance at BO_3 (Å)

(B)

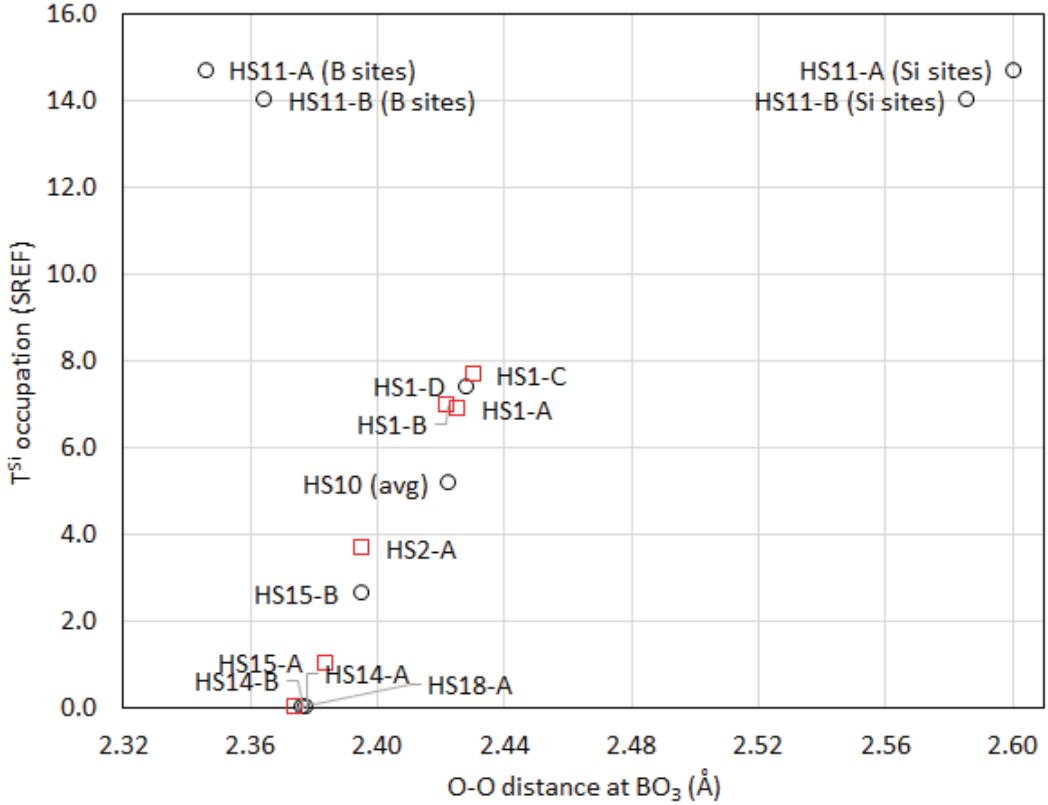
16.0
14.0
12.0
10.0
8.0
6.0
4.0
2.0
0.0
T^{Si} occupation (SREF)
HS11-A (B sites)
HS11-B (B sites)
HS11-A (Si sites)
HS11-B (Si sites)
HS1-D
HS1-C
HS1-A
HS1-B
HS10 (avg)
HS2-A
HS15-B
HS15-A
HS14-B
HS14-A
HS18-A
2.32
2.36
2.40
2.44
2.48
2.52
2.56
2.60
O-O distance at BO_3 (Å)

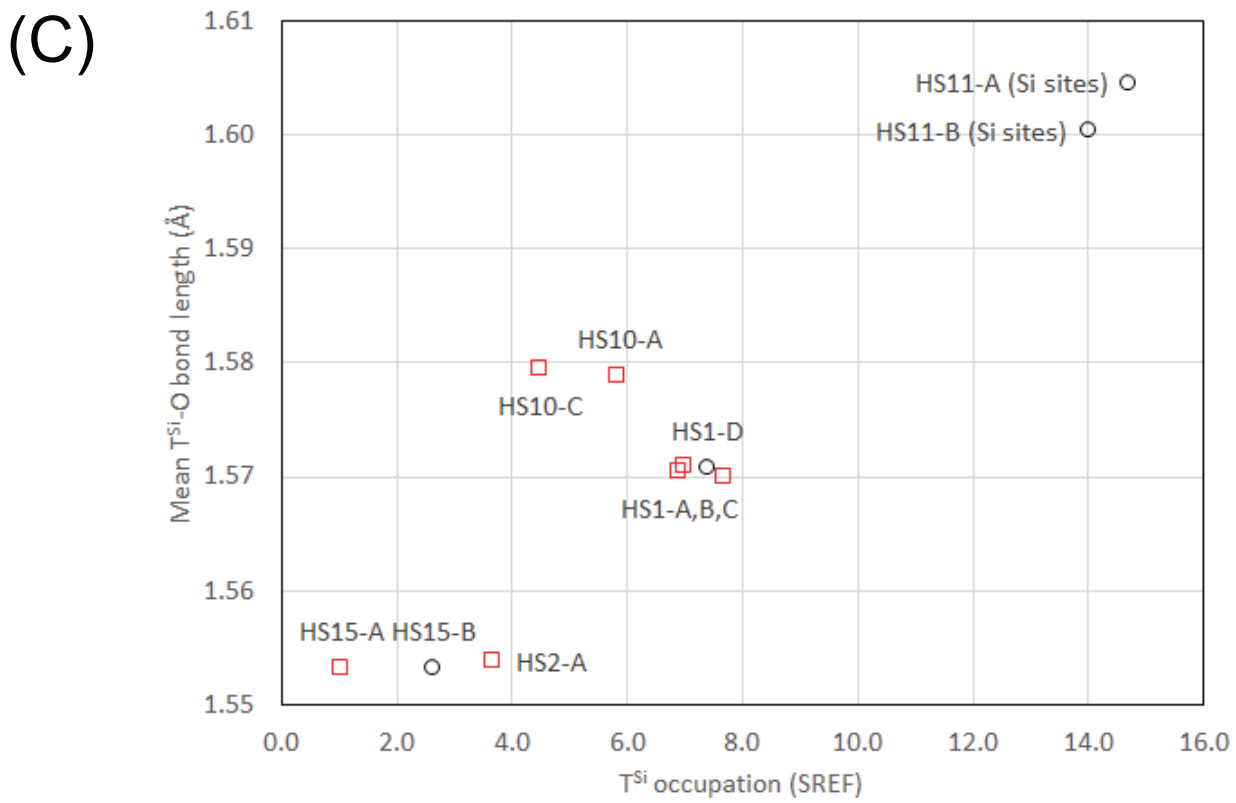
(C)
1.61
1.60
1.59
1.58
1.57
1.56
1.55
Mean T^Si-O bond length (Å)
HS11-A (Si sites)
HS11-B (Si sites)
HS10-A
HS10-C
HS1-D
HS1-A,B,C
HS15-A
HS15-B
HS2-A
0.0
2.0
4.0
6.0
8.0
10.0
12.0
14.0
16.0
T^Si occupation (SREF)

FIG. 7.

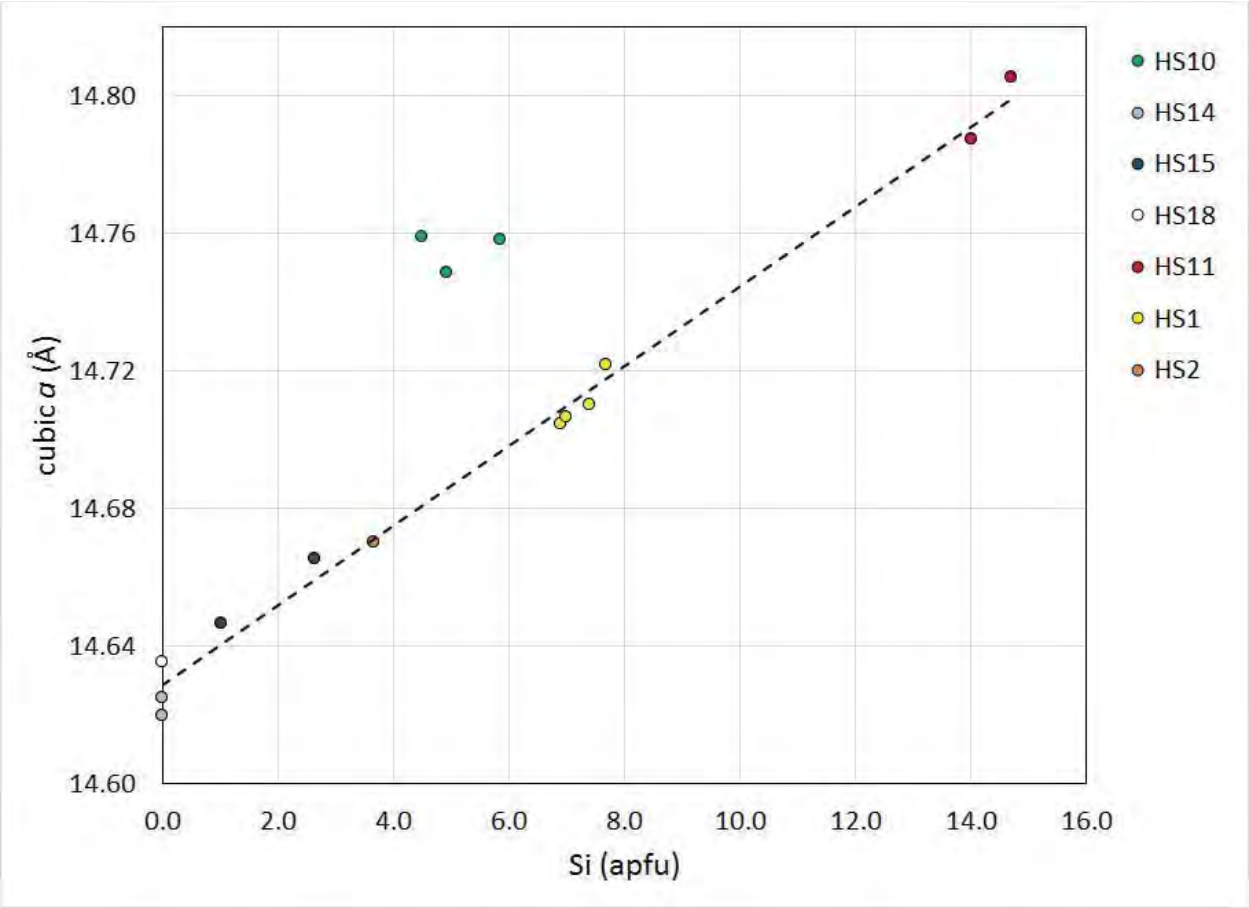
14.80
14.76
14.72
14.68
14.64
14.60
cubic a (Å)
0.0
2.0
4.0
6.0
8.0
10.0
12.0
14.0
16.0
Si (apfu)
HS10
HS14
HS15
HS18
HS11
HS1
HS2

FIG. 8.

This is a preprint, the final version is subject to change, of the American Mineralogist (MSA)
Cite as Authors (Year) Title. American Mineralogist, in press.
DOI: https://doi.org/10.2138/am-2018-6563

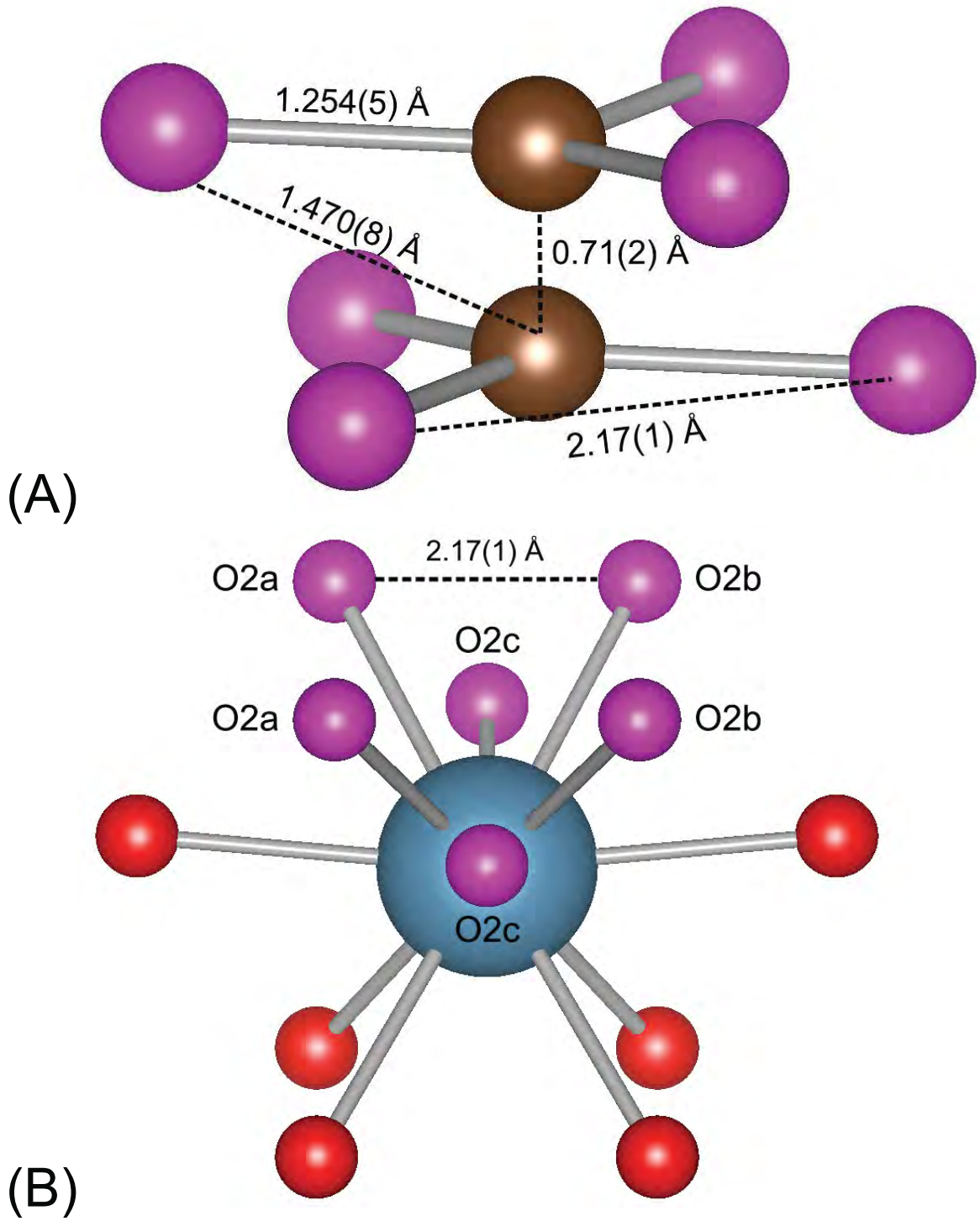

FIG. 9.

This is a preprint, the final version is subject to change, of the American Mineralogist (MSA)
Cite as Authors (Year) Title. American Mineralogist, in press.
DOI: https://doi.org/10.2138/am-2018-6563

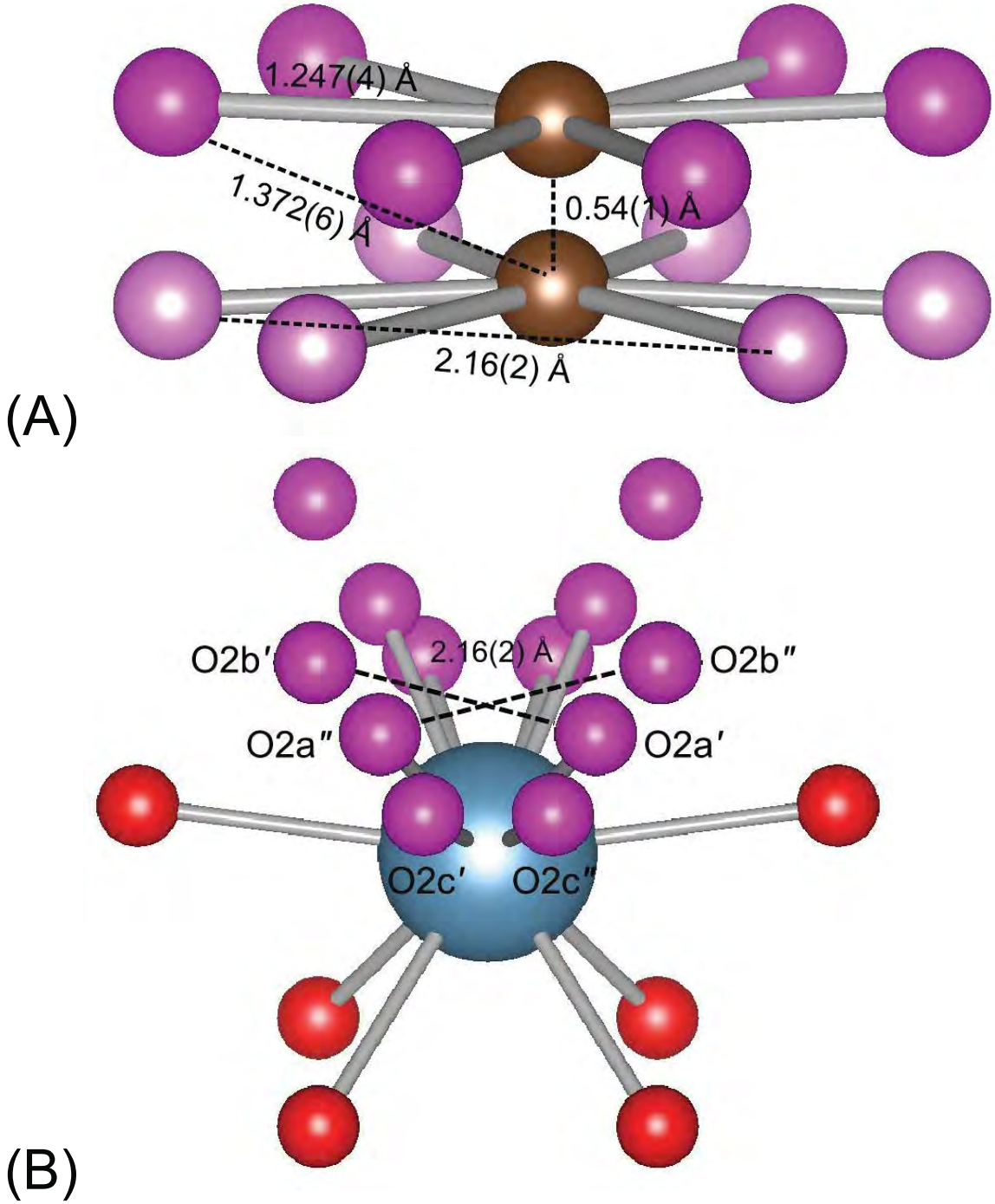

This is a preprint, the final version is subject to change, of the American Mineralogist (MSA)
Cite as Authors (Year) Title. American Mineralogist, in press.
DOI: https://doi.org/10.2138/am-2018-6563

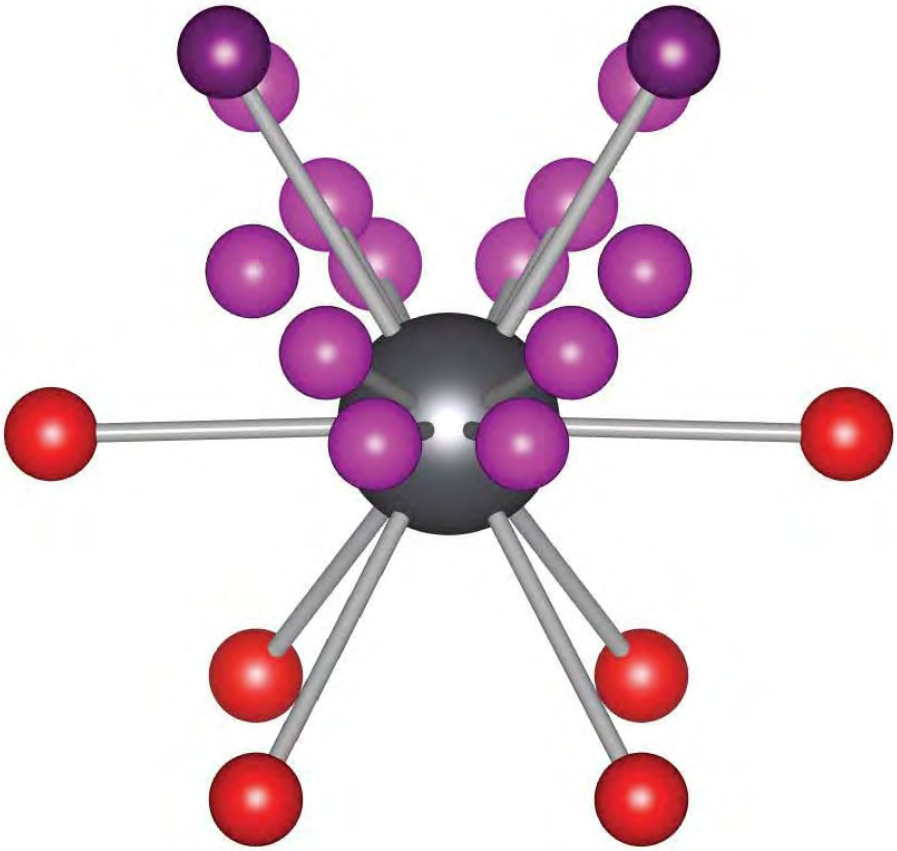

(C)

FIG. 10.

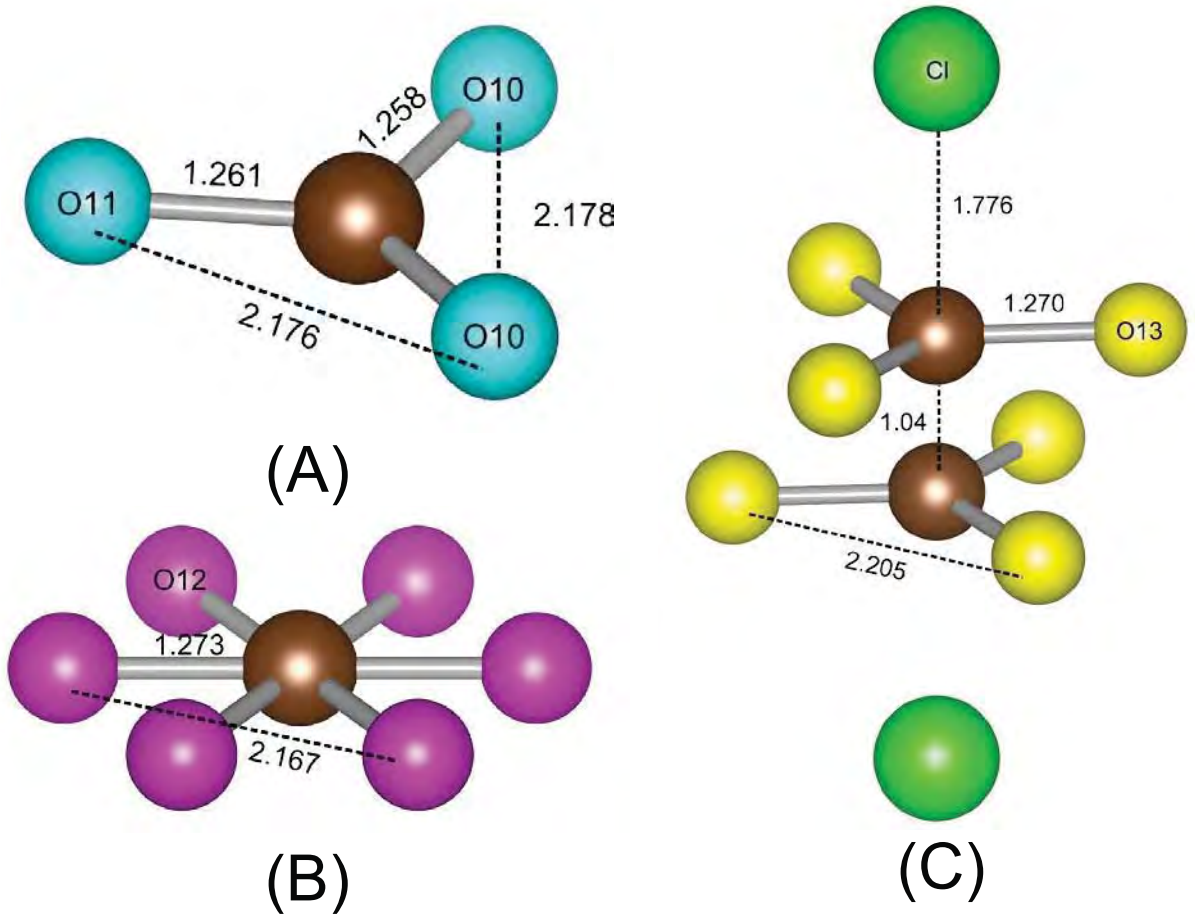
O10
1.258
1.261
O11
2.178
2.176
O10
(A)
O12
1.273
2.167
(B)
Cl
1.776
1.270
O13
1.04
2.205
(C)

FIG. 11.

This is a preprint, the final version is subject to change, of the American Mineralogist (MSA)
Cite as Authors (Year) Title. American Mineralogist, in press.
DOI: https://doi.org/10.2138/am-2018-6563

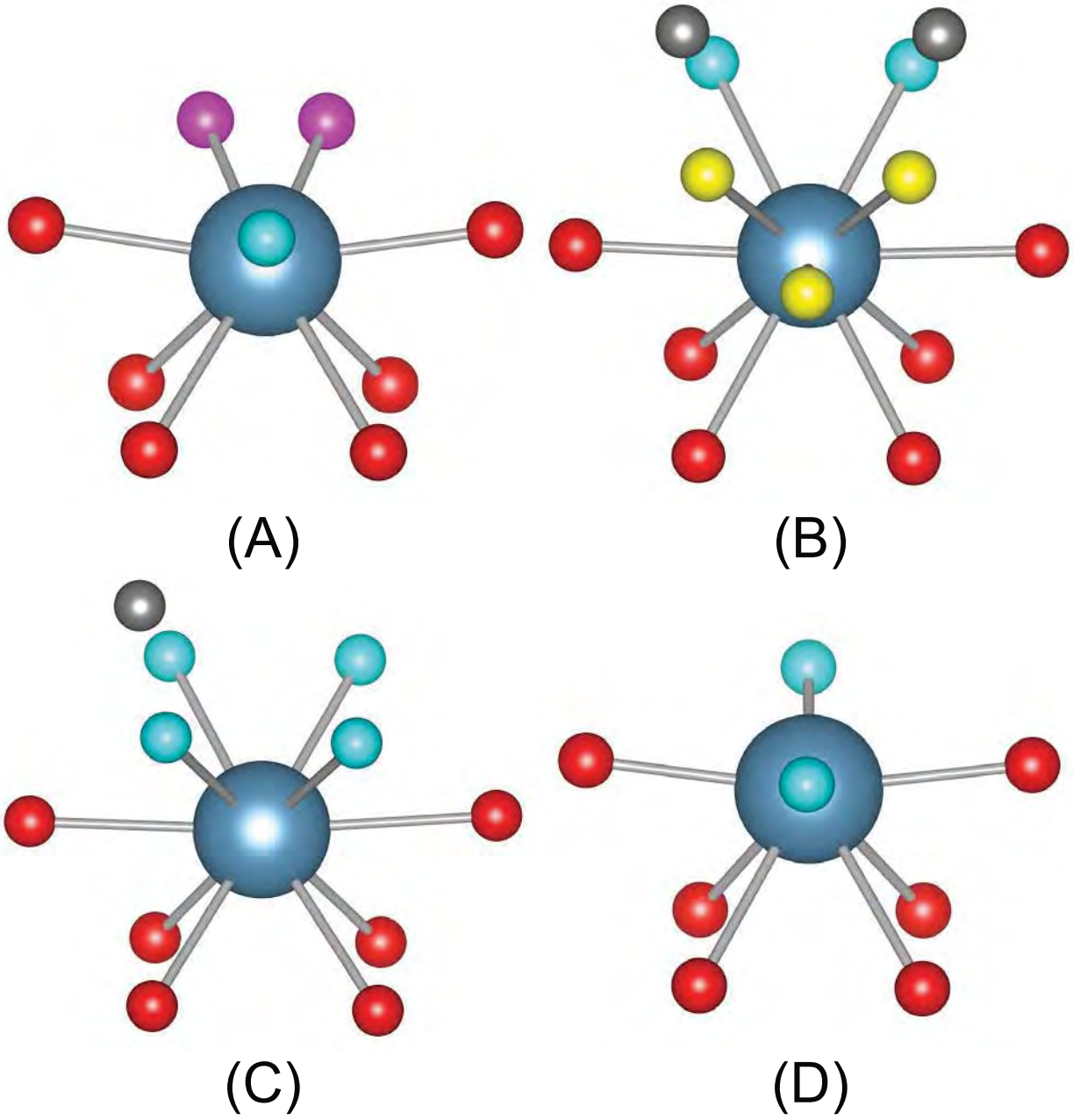

FIG. 12.

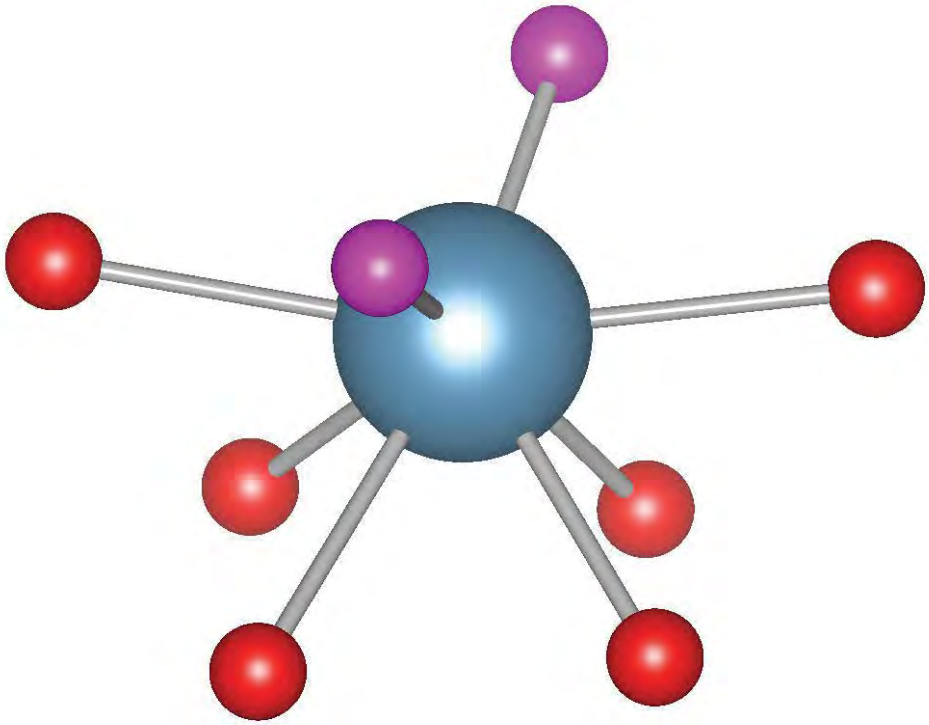

FIG. 13.

TABLE 1. Samples used in this study

Identifier	Species	Given locality	Source	Reference
HS1	sakhaite	Titovskoye B deposit, Sakha Republic, Russia	N.N. Pertsev	1
HS2	harkerite	Titovskoye B deposit, Sakha Republic, Russia	N.N. Pertsev	1
HS10	sakhaite-like mineral	Kombat Mine, Tsumeb, Namibia	NMNH 163833	2
HS11	harkerite	Camas Malag, Skye, Scotland	NMNH 106676	3
HS12	sakhaite	Solongo B deposit, Buryatia Republic, Russia	NMNH 153362	4
HS14	sakhaite	Titovskoye B deposit, Sakha Republic, Russia	NMNH 160105	1
HS15	sakhaite	Siberia, Russia*	NMNH 142161	–
HS18	sakhaite	Titovskoye B deposit, Sakha Republic, Russia	N.N. Pertsev #B-330 from P.M. Kartashov	1

NMNH – National Museum of Natural History (Smithsonian Institution). References for background on localities: [1] Ostrovskaya et al. (1966); [2] Dunn et al. (1990); [3] Tilley (1951); [4] Malinko and Kuznetsova (1973).

*No other locality information available.

TABLE 6. Data measurement and refinement information for sakhaite and harkerite

	HS15-A	HS10-A	HS1-A	HS11-A	HS14-B
a (Å)	14.6466(3)	14.7579(3)	14.7044(9)	10.4397(4)	14.7103(3)
V (Å^3)	3142.0(8)	3214.2(3)	3179.4(6)	4854.4(6)	3183.2(3)
Space group	$Fd\bar{3}m$	$Fd\bar{3}m$	$Fd\bar{3}m$	$R\bar{3}m$	$Fd\bar{3}m$
Z	4	4	4	3/2	4
Radiation	Mo*K*α	Mo*K*α	Mo*K*α	Mo*K*α	Mo*K*α
Monochromator	graphite	graphite	graphite	graphite	graphite
Total F_o	7637	30797	5464	24073	8487
Unique F_o	209	417	324	2352	645
$F_o > 4\sigma F_o$	184	414	288	1576	522
R_{int}	0.0365(8)	0.024(5)	0.03(2)	0.07(3)	0.020(9)
L.s. parameters	34	45	39	167	31
R_1 for $F_o > 4\sigma F_o$	0.0293	0.0309	0.0400	0.0622	0.0539
R_1, all unique F_o	0.0340	0.0310	0.0443	0.1016	0.660
wR_2	0.0483	0.0777	0.0850	0.1554	0.1332
a	0.0000	0.0208	0.000	0.0493	0.0352
b	44.23	21.55	48.35	82.0	46.54
GooF (= *S*)	1.118	1.318	1.134	1.111	1.110

Note: $w = 1/[\sigma^2(F_o^2) + (a \times P)^2 + b \times P]$ where $P = [\mathrm{Max}\,(F_o^2, 0) + 2 \times F_c^2)]/3$

TABLE 7A. Atomic parameters for sakhaite and harkerite

		HS15-A	HS10-A	HS1-A	HS14-B
Ca	*x*	1/8	0.3658(1)	1/8	-0.12257(6)
	y	0.3776(1)	1/8	0.37647(8)	5/8
	z	1/8	1/8	1/8	1/8
	Occ	0.955(7)	0.984(2)	0.964(7)	0.984(8)
Pb	*x*		0.394(1)		
	y		1/8		
	z		1/8		
	Occ		0.016(2)		
Mg	*x*	0	¼	0	0
	y	½	¼	½	½
	z	0	0	0	0
	Occ	0.91(1)	0.99(1)	1	0.969(8) Mg+ 0.031 Fe
B	*x*	-0.0338(4)	0.2154(2)	-0.0352(5)	0.0335(2)
	y	0.2838(4)	0.0346(2)	0.2852(5)	0.7165(2)
	z	-0.0338(4)	0.0346(2)	-0.0352(5)	0.0335(2)
	Occ	0.94(3)	0.81(2)	0.794(4)	1
Si	*x*	-0.007(3)	0.2435(2)	-0.0073(3)	
	y	0.257(3)	0.0065(2)	0.2573(3)	
	z	-0.007(3)	0.0065(2)	-0.0073(3)	
	Occ	0.032(5)	0.183(5)	0.215(7)	
Al	*x*	1/8	1/8	1/8	
	y	1/8	1/8	1/8	
	z	1/8	1/8	1/8	
	Occ	0.032(5)	0.183(5)	0.215(7)	
C	*x*	¼	0.0108(3)	0.2360(5)	¼
	y	¼	0.5108(3)	0.2360(5)	¼
	z	0	0.0108(3)	0.0140(5)	0
O1	*x*	0.0046(1)	0.2552(1)	0.0054(1)	0.1100(1)
	y	0.3606(1)	-0.0052(1)	0.3613(2)	0.75493(9)
	z	0.0046(1)	0.1110(1)	0.0054(1)	-0.00493(9)
O2	*x*	0.2290(3)	0.0758(5)	0.2314(3)	0.2721(3)
	y	0.3321(4)	0.4575(5)	0.3358(4)	0.2721(3)
	z	0.0213 (3)	0.0019(8)	0.0186(3)	0.0825(4)
O3	*x*	0.056(4)	0.307(1)	0.0566(6)	
	y	0.194(4)	-0.057(1)	0.1934(6)	
	z	0.056(4)	-0.057(1)	0.0566(6)	
	Occ	0.032(5)	0.183(5)	0.215(7)	
Cl / OW	*x*	1/8	0.155(2)	0.097(1)	0.1511(9)
	y	1/8	0.655(2)	0.097(1)	0.1511(9)
	z	1/8	0.095(2)	0.097(1)	0.0989(9)
	Occ	0.73(3)	0.063(7)	0.125(7)	0.18(1)

TABLE 7B. Atomic parameters for sakhaite and harkerite

		HS11-A
Ca1	*x*	0.83989(6)
	y	0.6798(1)
	z	0.35310(2)
	Occ	1.0
Ca2	*x*	0.17329(7)
	y	0.3466(1)
	z	0.14466(2)
	Occ	1.0
Ca3	*x*	0.16140(7)
	y	0.3228(2)
	z	0.39677(2)
	Occ	1.0
Ca4	*x*	0.82891(7)
	y	0.6578(1)
	z	0.10574(2)
	Occ	1.0
Mg1	*x*	1/3
	y	1/6
	z	1/6
	Occ	0.944(9)
Fe1	*x*	1/3
	y	1/6
	z	1/6
	Occ	0.056(9)
Mg2	*x*	2/3
	y	5/6
	z	1/3
	Occ	0.954(9)
Fe2	*x*	2/3
	y	5/6
	z	1/3
	Occ	0.046(9)
Mg3	*x*	0
	y	0
	z	0.24846(5)
	Occ	0.96(1)
Fe3	*x*	0
	y	0
	z	0.24846(5)
	Occ	0.04(1)
Si1	*x*	0.84389(9)
	y	0.6877(2)

	z	0.29127(3)
	Occ	0.863(6)
Si2	*x*	0
	y	0
	z	0.12970(6)
	Occ	0.88(1)
Al1	*x*	0
	y	0
	z	0.06421(5)
	Occ	1.06(1)
B1A	*x*	0.880(2)
	y	0.759(5)
	z	0.2968(7)
	Occ	0.137(6)
B2A	*x*	0
	y	0
	z	0.141(2)
	Occ	0.12(1)
B1	*x*	0.1177(3)
	y	0.2354(6)
	z	0.20037(9)
	Occ	0.946(4)
B2	*x*	0
	y	0
	z	0.3541(2)
	Occ	0.959(6)
Si1A	*x*	0.151(1)
	y	0.303(3)
	z	0.2058(4)
	Occ	0.054(4)
Si2A	*x*	0
	y	0
	z	0.369(1)
	Occ	0.041(6)
Al1A	*x*	0
	y	0
	z	0.437(1)
	Occ	0.050(8)
C1	*x*	0.1896(3)
	y	0.3792(6)
	z	0.08602(9)
C2	*x*	0
	y	0
	z	0
C3	*x*	0
	y	0

	z	0.4884(3)
O1	*x*	0.9335(3)
	y	0.3551(3)
	z	0.14523(5)
O2	*x*	0.0512(3)
	y	0.6513(3)
	z	0.35838(5)
O3	*x*	0.0925(2)
	y	0.1851(4)
	z	0.22471(7)
O4	*x*	0.9013(2)
	y	0.8026(4)
	z	0.26750(6)
O5	*x*	0.0752(2)
	y	0.1504(4)
	z	0.35455(6)
O6	*x*	0.9170(2)
	y	0.8340(4)
	z	0.13954(7)
Cl	*x*	0
	y	0
	z	0.4555(1)
	Occ	0.42(1)
O8	*x*	0.9071(2)
	y	0.8141(5)
	z	0.05426(8)
	Occ	0.863(6)
O9	*x*	0
	y	0
	z	0.0980(1)
	Occ	0.88(1)
O10	*x*	0.0734(4)
	y	0.3565(4)
	z	0.09742(7)
O11	*x*	0.2166(3)
	y	0.4333(5)
	z	0.06342(7)
O12	*x*	0.878(1)
	y	0
	z	0
O13	*x*	0.0702(4)
	y	0.1404(8)
	z	0.4881(2)
O14	*x*	0.245(7)
	y	0.49(1)
	z	0.213(2)

	Occ	0.054(4)
O15	*x*	0
	y	0
	z	0.403(2)
	Occ	0.041(6)

TABLE 8A. Atomic displacement parameters for sakhaite and harkerite

		HS15-A	HS10-A	HS1-A	HS14-B
Ca	U_{11}	0.0159(3)	0.0164 (5)	0.0158(3)	0.0327(4)
	U_{22}	0.033(1)	0.0123(2)	0.0461(6)	0.0158(2)
	U_{33}	0.0159(3)	0.0123(2)	0.0158(3)	0.0158(2)
	U_{12}	0	0	0	0
	U_{13}	-0.0051(3)	0	-0.0034(3)	0
	U_{23}	0	0.0019(2)	0	-0.0070(2)
	U_{eq}	0.0216(3)	0.0137(2)	0.0259(3)	0.0214(2)
Pb	U_{11}		0.012(5)		
	U_{22}		0.040(5)		
	U_{33}		0.040(5)		
	U_{12}		0		
	U_{13}		0		
	U_{23}		0.005(4)		
	U_{eq}		0.030(4)		
Mg	U_{11}	0.0074(6)	0.0079(4)	0.0090(5)	0.0070(4)
	U_{22}	0.0074(6)	0.0079(4)	0.0090(5)	0.0070(4)
	U_{33}	0.0074(6)	0.0079(4)	0.0090(5)	0.0070(4)
	U_{12}	-0.0005(5)	-0.0006(2)	0.0009(4)	-0.0006(2)
	U_{13}	-0.0005(5)	0.0006(2)	0.0009(4)	-0.0006(2)
	U_{23}	-0.0005(5)	0.0006(2)	0.0009(4)	-0.0006(2)
	U_{eq}	0.0074(6)	0.0079(4)	0.0090(5)	0.0070(4)
B	U_{11}	0.014(2)	0.009(1)	0.018(2)	0.0118(8)
	U_{22}	0.014(2)	0.009(1)	0.018(2)	0.0118(8)
	U_{33}	0.014(2)	0.009(1)	0.018(2)	0.0118(8)
	U_{12}	-0.003(2)	-0.001(1)	-0.004(2)	-0.0022(6)
	U_{13}	-0.003(2)	-0.001(1)	0.004(2)	0.0022(6)
	U_{23}	-0.003(2)	0.001(1)	-0.004(2)	-0.0022(6)
	U_{eq}	0.014(2)	0.009(1)	0.018(2)	0.0118(8)
Si	U_{11}	0.014(5)	0.008(1)	0.006(1)	
	U_{22}	0.014(5)	0.008(1)	0.006(1)	
	U_{33}	0.014(5)	0.008(1)	0.006(1)	
	U_{12}	-0.003(2)	-0.001(1)	0.002(1)	
	U_{13}	-0.003(2)	-0.001(1)	-0.002(1)	
	U_{23}	-0.003(2)	0.001(1)	0.002(1)	
	U_{eq}	0.014(5)	0.008(1)	0.006(1)	
Al	U_{eq}	0.006	0.015	0.006	

C	U_{11}	0.053(4)	0.014(1)	0.026(3)	0.057(4)
	U_{22}	0.053(4)	0.014(1)	0.026(3)	0.057(4)
	U_{33}	0.053(4)	0.014(1)	0.026(3)	0.057(4)
	U_{12}	-0.039(5)	0.006(2)	0.010(3)	0.050(4)
	U_{13}	0.039(5)	0.006(2)	-0.010(3)	-0.050(4)
	U_{23}	0.039(5)	0.006(2)	-0.010(3)	-0.050(4)
	U_{eq}	0.053(4)	0.014(1)	0.026(3)	0.057(4)
O1	U_{11}	0.026(1)	0.0239(5)	0.0384(9)	0.0091(6)
	U_{22}	0.015(1)	0.0239(5)	0.015(1)	0.0230(5)
	U_{33}	0.026(1)	0.0105(6)	0.0384(9)	0.0230(5)
	U_{12}	-0.003(1)	-0.0053(5)	-0.0004(6)	-0.0037(3)
	U_{13}	0.003(1)	-0.0041(3)	0.006(1)	0.0037(3)
	U_{23}	-0.003(1)	0.0041(3)	-0.0004(6)	-0.0030(6)
	U_{eq}	0.022(1)	0.0194(4)	0.0304(7)	0.0184(4)
O2	U_{11}	0.087(4)	0.040(4)	0.068(3)	0.067(3)
	U_{22}	0.031(3)	0.056(5)	0.032(3)	0.067(3)
	U_{33}	0.087(4)	0.044(3)	0.068(3)	0.038(3)
	U_{12}	0.016(2)	0.037(4)	-0.017(2)	-0.027(3)
	U_{13}	0.047(5)	0.006(4)	0.022(3)	-0.021(2)
	U_{23}	-0.016(2)	-0.006(5)	0.017(2)	-0.021(2)
	U_{eq}	0.068(2)	0.047(3)	0.056(2)	0.057(2)
O3	U_{11}	0.05(5)	0.030(4)	0.023(4)	
	U_{22}	0.05(5)	0.030(4)	0.023(4)	
	U_{33}	0.05(5)	0.030(4)	0.023(4)	
	U_{12}	0.04(3)	-0.010(3)	0.010(3)	
	U_{13}	-0.04(3)	-0.010(3)	-0.010(3)	
	U_{23}	0.04(3)	0.010(3)	0.010(3)	
	U_{eq}	0.05(5)	0.030(4)	0.023(4)	
Cl / OW	U_{11}		0.4(1)	0.089(9)	0.13(1)
	U_{22}		0.4(1)	0.089(9)	0.13(1)
	U_{33}		0.4(1)	0.089(9)	0.13(1)
	U_{12}		-0.17(6)	-0.013(7)	-0.030(7)
	U_{13}		0.17(6)	-0.013(7)	0.030(7)
	U_{23}		0.17(6)	-0.013(7)	0.030(7)
	U_{eq}	0.015	0.4(1)	0.089(9)	0.13(1)

TABLE 8B. Atomic displacement parameters for sakhaite and harkerite

		HS11-A
Ca1	U_{11}	0.0098(4)
	U_{22}	0.0179(5)
	U_{33}	0.0170(5)
	U_{12}	0.0090(3)
	U_{13}	-0.0028(2)
	U_{23}	-0.0056(4)
	U_{eq}	0.0140(3)
Ca2	U_{11}	0.0164(4)
	U_{22}	0.0220(6)
	U_{33}	0.0223(5)
	U_{12}	0.0110(3)
	U_{13}	-0.0048(2)
	U_{23}	-0.0096(4)
	U_{eq}	0.0196(3)
Ca3	U_{11}	0.0168(4)
	U_{22}	0.0253(6)
	U_{33}	0.0238(5)
	U_{12}	0.0126(3)
	U_{13}	-0.0001(2)
	U_{23}	-0.0002(4)
	U_{eq}	0.0210(3)
Ca4	U_{11}	0.0132(4)
	U_{22}	0.0209(6)
	U_{33}	0.0150(4)
	U_{12}	0.0105(3)
	U_{13}	-0.0055(2)
	U_{23}	-0.0110(4)
	U_{eq}	0.0155(3)
Mg1	U_{11}	0.007(1)
	U_{22}	0.0075(8)
	U_{33}	0.0052(9)
	U_{12}	0.0035(6)
	U_{13}	-0.0002(7)
	U_{23}	-0.0001(3)
	U_{eq}	0.0066(6)
Fe1	U_{11}	0.007(1)
	U_{22}	0.0075(8)

	U_{33}	0.0052(9)
	U_{12}	0.0035(6)
	U_{13}	-0.0002(7)
	U_{23}	-0.0001(3)
	U_{eq}	0.0066(6)
Mg2	U_{11}	0.004(1)
	U_{22}	0.0066(8)
	U_{33}	0.0073(9)
	U_{12}	0.0020(5)
	U_{13}	-0.0021(7)
	U_{23}	-0.0011(3)
	U_{eq}	0.0063(6)
Fe2	U_{11}	0.004(1)
	U_{22}	0.0066(8)
	U_{33}	0.0073(9)
	U_{12}	0.0020(5)
	U_{13}	-0.0021(7)
	U_{23}	-0.0011(3)
	U_{eq}	0.0063(6)
Mg3	U_{11}	0.0061(9)
	U_{22}	0.0061(9)
	U_{33}	0.006(1)
	U_{12}	0.0030(5)
	U_{13}	0
	U_{23}	0
	U_{eq}	0.0061(8)
Fe3	U_{11}	0.007(2)
	U_{22}	0.0061(9)
	U_{33}	0.006(1)
	U_{12}	0.0030(5)
	U_{13}	0
	U_{23}	0
	U_{eq}	0.0061(8)
Si1	U_{11}	0.0049(5)
	U_{22}	0.0052(7)
	U_{33}	0.0059(6)
	U_{12}	0.0026(4)
	U_{13}	-0.0003(2)
	U_{23}	-0.0007(5)
	U_{eq}	0.0053(3)

DOI: https://doi.org/10.2138/am-2018-6563

Si2	U_{11}	0.0059(7)
	U_{22}	0.0059(7)
	U_{33}	0.003(1)
	U_{12}	0.0030(4)
	U_{13}	0
	U_{23}	0
	U_{eq}	0.0057(7)
Al1	U_{11}	0.0100(8)
	U_{22}	0.0100(8)
	U_{33}	0.009(1)
	U_{12}	0.0050(4)
	U_{13}	0
	U_{23}	0
	U_{eq}	0.0098(7)
B1A	U_{11}	0.0049(5)
	U_{22}	0.0052(7)
	U_{33}	0.0059(6)
	U_{12}	0.0026(4)
	U_{13}	-0.0003(2)
	U_{23}	-0.0007(5)
	U_{eq}	0.0053(3)
B2A	U_{11}	0.0059(7)
	U_{22}	0.0059(7)
	U_{33}	0.003(1)
	U_{12}	0.0030(4)
	U_{13}	0
	U_{23}	0
	U_{eq}	0.0051(7)
B1	U_{11}	0.0049(5)
	U_{22}	0.0052(7)
	U_{33}	0.0059(6)
	U_{12}	0.0026(4)
	U_{13}	-0.003(2)
	U_{23}	-0.007(5)
	U_{eq}	0.0053(3)
B2	U_{11}	0.0059(7)
	U_{22}	0.0059(7)
	U_{33}	0.003(1)
	U_{12}	0.030(4)
	U_{13}	0

	U_{23}	0
	U_{eq}	0.0051(7)
Si1A	U_{11}	0.0049(5)
	U_{22}	0.0052(7)
	U_{33}	0.0059(6)
	U_{12}	0.0026(4)
	U_{13}	-0.0003(2)
	U_{23}	-0.0007(5)
	U_{eq}	0.0053(3)
Si2A	U_{11}	0.0059(7)
	U_{22}	0.0059(7)
	U_{33}	0.003(1)
	U_{12}	0.0030(4)
	U_{13}	0
	U_{23}	0
	U_{eq}	0.0051(7)
Al1A	U_{11}	0.010(2)
	U_{22}	0.010(2)
	U_{33}	0.0092(8)
	U_{12}	0.005(1)
	U_{13}	0
	U_{23}	0
	U_{eq}	0.010(2)
C1	U_{11}	0.013(2)
	U_{22}	0.015(2)
	U_{33}	0.012(2)
	U_{12}	0.008(1)
	U_{13}	-0.0002(9)
	U_{23}	-0.000(2)
	U_{eq}	0.0130(9)
C2	U_{11}	0.009(3)
	U_{22}	0.009(3)
	U_{33}	0.013(5)
	U_{12}	0.004(2)
	U_{13}	0
	U_{23}	0
	U_{eq}	0.010(2)
C3	U_{11}	0.009(4)
	U_{22}	0.009(4)
	U_{33}	0.019(8)

	U_{12}	0.004(2)
	U_{13}	0
	U_{23}	0
	U_{eq}	0.012(3)
O1	U_{11}	0.036(2)
	U_{22}	0.015(1)
	U_{33}	0.019(1)
	U_{12}	0.012(1)
	U_{13}	0.010(1)
	U_{23}	0.013(1)
	U_{eq}	0.0234(7)
O2	U_{11}	0.021(1)
	U_{22}	0.014(1)
	U_{33}	0.021(1)
	U_{12}	0.011(1)
	U_{13}	0.006(1)
	U_{23}	0.013(1)
	U_{eq}	0.0176(6)
O3	U_{11}	0.016(1)
	U_{22}	0.013(1)
	U_{33}	0.021(2)
	U_{12}	0.0066(9)
	U_{13}	0.0058(7)
	U_{23}	0.012(1)
	U_{eq}	0.0167(8)
O4	U_{11}	0.032(2)
	U_{22}	0.008(2)
	U_{33}	0.009(1)
	U_{12}	0.0042(8)
	U_{13}	0.0023(6)
	U_{23}	0.005(1)
	U_{eq}	0.0191(8)
O5	U_{11}	0.011(1)
	U_{22}	0.010(2)
	U_{33}	0.017(2)
	U_{12}	0.0048(8)
	U_{13}	0.0042(7)
	U_{23}	0.008(1)
	U_{eq}	0.0127(7)
O6	U_{11}	0.058(2)

	U_{22}	0.006(2)
	U_{33}	0.009(2)
	U_{12}	0.0032(9)
	U_{13}	0.0003(7)
	U_{23}	0.000(1)
	U_{eq}	0.030(1)
Cl	U_{11}	0.028(2)
	U_{22}	0.028(2)
	U_{33}	0.018(3)
	U_{12}	0.014(1)
	U_{13}	0
	U_{23}	0
	U_{eq}	0.025(2)
O8	U_{11}	0.022(2)
	U_{22}	0.006(2)
	U_{33}	0.027(2)
	U_{12}	0.0029(9)
	U_{13}	-0.0042(8)
	U_{23}	-0.008(2)
	U_{eq}	0.0200(10)
O9	U_{11}	0.031(3)
	U_{22}	0.031(3)
	U_{33}	0.009(3)
	U_{12}	0.016(2)
	U_{13}	0
	U_{23}	0
	U_{eq}	0.024(2)
O10	U_{11}	0.020(2)
	U_{22}	0.042(2)
	U_{33}	0.055(2)
	U_{12}	0.007(2)
	U_{13}	0.023(2)
	U_{23}	-0.007(2)
	U_{eq}	0.043(1)
O11	U_{11}	0.051(2)
	U_{22}	0.031(3)
	U_{33}	0.013(2)
	U_{12}	0.015(1)
	U_{13}	0.0035(9)
	U_{23}	0.007(2)

	U_{eq}	0.034(1)
O12	U_{11}	0.035(4)
	U_{22}	0.047(6)
	U_{33}	0.062(6)
	U_{12}	0.023(3)
	U_{13}	0.014(2)
	U_{23}	0.028(5)
	U_{eq}	0.047(3)
O13	U_{11}	0.017(3)
	U_{22}	0.006(3)
	U_{33}	0.032(4)
	U_{12}	0.003(2)
	U_{13}	0.001(1)
	U_{23}	0.003(3)
	U_{eq}	0.020(2)
O14	U_{eq}	0.05(3)
O15	U_{eq}	0.05

TABLE 9A. Selected bond lengths (Å) for sakhaite and harkerite

			HS1-A	HS15-A	HS14-B
Mg	O1	× 6	2.043(3)	2.045(2)	2.050(2)
Ca	O2	× 2	2.293(6)	2.248(6)	2.228(5)
	O1	× 2	2.498(3)	2.507(2)	2.496(2)
	O1	× 4	2.5950(8)	2.5739(9)	2.5727(6)
	O2	× 4	2.703(2)	2.722(2)	2.718(2)
<[9]Ca-O>			2.564	2.556	2.550
C	O2	× 3	1.254(5)	1.281(5)	1.290(5)
B	O1	× 3	1.401(2)	1.376(2)	1.373(2)
Si	O1	× 3	1.551(4)	1.53(4)	
	O3		1.63(2)	1.62(13)	
<Si-O>			1.570	1.553	
Al	O3	× 3	1.74(2)	1.74(10)	

TABLE 9B. Selected bond lengths (Å) for sakhaite and harkerite

	HS10-A		
Mg	O1	× 6	2.054(2)
Ca	O2	× 4	2.379(10)
	O2	× 4	2.394(9)
	O1	× 2	2.524(2)
	O1	× 4	2.530(1)
$<^{[8]}$Ca-O>			2.493
Pb	O2	× 4	2.17(1)
	O2	× 4	2.279(10)
	O1	× 2	2.502(2)
	O1	× 4	2.81(2)
	O3	× 2*	2.80(2)
$<^{[8-10]}$Pb-O>			2.60
C	O2	× 3	1.247(4)
B	O1	× 3	1.400(2)
Si	O1	× 3	1.561(3)
	O3		1.63(2)
<Si-O>			1.579
Al	O3	× 3	1.73(2)

*partial occupation of each O3 site = 0.183(2), which is taken into account calculating the mean Pb-O distance.

TABLE 9C. Selected bond lengths (Å) for sakhaite and harkerite

HS11-A											
Mg1	O1	× 4	2.030(2)	Ca4	O10	× 2	2.346(3)	Si1A	O3		1.44(2)
	O6	× 2	2.058(4)		O4		2.352(4)		O1	× 2	1.52(1)
<Mg1-O>			2.039		O6		2.358(4)		O14		1.73(12)
					O3	× 2	2.553(1)	<Si1A-O>			1.55
Mg2	O5	× 2	1.982(3)		O1	× 2	2.628(3)				
	O2	× 4	2.106(2)	<[8]Ca4-O>			2.471	Si2A	O5	× 3	1.55(3)
<Mg2-O>			2.064						O15		1.71(10)
								<Si2A-O>			1.59
Mg3	O4	× 3	2.036(4)	Si1	O2	× 2	1.601(2)				
	O3	× 3	2.072(4)		O4		1.604(4)	Al1A	O15	× 3	1.79(11)
<Mg3-O>			2.054		O8		1.648(4)		O14		1.81(12)
				<Si1-O>			1.613	<Al1A-O>			1.80
Ca1	O12	× 2	2.357(6)								
	O11		2.378(4)	Si2	O6		1.584(4)	B1A	O2	× 2	1.49(2)
	O2	× 2	2.384(3)		O9		1.631(8)		O4		1.56(3)
	O5	× 2	2.510(1)	<Si2-O>			1.596	<B1A-O>			1.51
	O2	× 2	2.675(3)								
<[8]Ca1-O>			2.484	Al1	O9		1.737(7)	B2A	O6	× 3	1.502(6)
					O8	× 3	1.757(4)				
Ca2	O13		2.383(8)	<Al1-O>			1.752				
	O1	× 2	2.550(3)								
	O13	× 2	2.566(2)	B1	O3		1.332(6)				
	O1	× 2	2.622(3)		O1	× 2	1.355(4)				
	O10	× 2	2.666(4)	<B1-O>			1.348				
	O6	× 2	2.727(1)								
<[9½]Ca2-O>			2.620	B2	O5	× 3	1.360(4)				
Ca3	O2	× 2	2.607(3)	C1	O10	× 2	1.258(4)				
	O11	× 2	2.610(2)		O11		1.261(6)				
	O10	× 2	2.631(4)	<C1-O>			1.259				
	O5		2.673(4)								
	O4	× 2	2.705(1)	C2	O12	× 3	1.273(10)				
	O3		2.732(4)								
<[10]Ca3-O>			2.651	C3	O13	× 3	1.270(8)				

TABLE 10. Chemical formulae as determined by structure refinement (SREF) versus electron microprobe analyses (EMPA), for crystals where both data sets are available.

Crystal	SREF	EMPA (average)
HS1-D	$Ca_{46.4(3)}$ $Mg_{15.9(2)}$ $[Al_{1.85(5)}$ $Si_{7.4(2)}]$ $B_{25.4(9)}$ C_{16} $O_{151.4(2)}$ $(HCl)_{3.7(2)}$	$[Ca_{47.97(2)}$ $Na_{0.01(1)}$ $K_{0.01(1)}]$ $[Mg_{15.1(2)}$ $Fe_{0.52(2)}$ $Mn_{0.03(3)}]$ $[Al_{2.2(3)}$ $Si_{7.0(4)}]$ $B_{24.6(3)}$ C_{16} $O_{148.5(7)}$ $(OH)_{2.3(7)}$ $F_{0.55(4)}$ $(HCl)_{3.54(7)}$
HS14-A	$Ca_{46.2(3)}$ $[Mg_{15.8(2)}$ $Fe_{0.2(2)}]$ B_{32} C_{16} O_{144} $(HCl)_{5.8(3)}$	$[Ca_{47.1(1.3)}$ $Na_{0.03(3)}$ $K_{0.02(1)}]$ $[Mg_{15.17(4)}$ $Fe_{0.73(4)}$ $Mn_{0.08(2)}]$ $[Al_{0.49(4)}$ $Si_{1.0(2)}]$ $B_{30.8(2)}$ C_{16} $O_{143(1)}$ $(OH)_{1.7(8)}$ $F_{0.58(2)}$ $(HCl)_{4.82(7)}$
HS14-B	$Ca_{47.0(4)}$ $[Mg_{15.6(2)}$ $Fe_{0.4(2)}]$ B_{32} C_{16} O_{144} $(HCl)_{5.7(3)}$	$[Ca_{47.4(3)}$ $Na_{0.04(1)}]$ $[Mg_{15.10(3)}$ $Fe_{0.83(2)}$ $Mn_{0.07(1)}]$ $[Al_{0.13(2)}$ $Si_{0.24(2)}]$ $B_{31.70(2)}$ C_{16} $O_{143.0(5)}$ $OH_{0.6(4)}$ $F_{0.64(3)}$ $(HCl)_{5.14(3)}$
HS15-B	$Ca_{46.8(3)}$ $[Mg_{14.4(2)}$ $Fe_{1.6(2)}]$ $[Al_{0.66(3)}$ $Si_{2.6(2)}]$ $B_{29.4(1)}$ C_{16} $O_{146.6(1)}$ $(HCl)_{5.1(3)}$	$[Ca_{46.8(6)}$ $Na_{0.01(1)}$ $Sr_{0.039(2)}$ $REE_{0.04(1)}]$ $[Mg_{13.9(2)}$ $Fe_{1.59(8)}$ $Mn_{0.52(3)}]$ $[Al_{1.0(1)}$ $Si_{2.5(3)}]$ $B_{29.1(3)}$ $S_{0.11(1)}$ $P_{0.02(2)}$ C_{16} $O_{144(2)}$ $(OH)_{3(1)}$ $F_{0.47(6)}$ $(HCl)_{3.8(1)}$
HS11-A	Ca_{48} $[Mg_{15.5(2)}$ $Fe_{0.5(2)}]$ $[Al_{3.76(3)}$ $Si_{15.0(2)}]$ $B_{17.0(2)}$ C_{16} $O_{159.0(2)}$ $(HCl)_{1.56(5)}$	$Ca_{46.5(2)}$ $[Mg_{15.19(3)}$ $Fe_{0.76(3)}$ $Mn_{0.04(1)}]$ $[Al_{3.12(3)}$ $Si_{13.6(3)}]$ $B_{18.6(2)}$ C_{16} $O_{151.0(3)}$ $(OH)_{5.8(3)}$ $F_{0.50(7)}$ $(HCl)_{2.14(5)}$
HS11-B	Ca_{48} $[Mg_{15.4(2)}$ $Fe_{0.6(2)}]$ $[Al_{3.46(3)}$ $Si_{13.8(2)}]$ $B_{18.2(2)}$ C_{16} $O_{157.8(2)}$ $(HCl)_{1.14(4)}$	$[Ca_{47.1(3)}$ $Na_{0.03(2)}$ $K_{0.01(1)}]$ $[Mg_{15.25(1)}$ $Fe_{0.70(1)}$ $Mn_{0.05(2)}]$ $[Al_{2.88(3)}$ $Si_{12.4(2)}]$ $B_{19.8(2)}$ C_{16} $O_{151.6(5)}$ $(OH)_{4.1(5)}$ $F_{0.50(1)}$ $(HCl)_{2.08(5)}$
HS10 (avg.)	$[Ca_{47.51(8)}$ $Pb_{0.49(8)}]$ $Mg_{15.7(2)}$ $[Al_{1.29(5)}Si_{5.2(2)}]$ $B_{26.7(5)}$ C_{16} $O_{149.2(2)}$ $(H_2O)_{2.8(5)}$	$[Ca_{47.2(3)}$ $Na_{0.01(1)}$ $Pb_{0.5(1)}$ $Sr_{0.7(2)}$ $Ba_{0.01(1)}$ $REE_{0.13(5)}]$ $[Mg_{15.5(3)}$ $Mn_{0.26(3)}]$ $[Al_{1.3(2)}$ $Si_{5.4(5)}]$ $B_{26.6(4)}$ C_{16} $S_{0.21(4)}$ $O_{147.1(7)}$ $(OH)_{1.5(5)}$ $F_{0.47(6)}$ $(HCl)_{0.25(4)}$